

Unified wave field imaging of inhomogeneous non-reciprocal media

Kees Wapenaar and Christian Reinicke

Delft University of Technology, P.O. Box 5048, 2600 GA Delft, The Netherlands

SUMMARY

Acoustic imaging methods often ignore multiple scattering. This may lead to false images in cases where multiple scattering is strong. Marchenko imaging has recently been introduced as a data-driven way to deal with internal multiple scattering. Promising results have been obtained with geophysical and ultrasonic data. Given the increasing interest in non-reciprocal materials, both for acoustic and electromagnetic applications, we propose to modify the Marchenko method for imaging of such materials.

We start by formulating a unified wave equation for non-reciprocal materials, exploiting the similarity between acoustic and electromagnetic wave phenomena. This unified wave equation forms the basis for deriving reciprocity theorems that interrelate wave fields in a non-reciprocal medium and its adjoint. Next, we reformulate these theorems for downgoing and upgoing wave fields. From these decomposed reciprocity theorems we derive representations of the Green's function inside the non-reciprocal medium, in terms of the reflection response at the surface and focusing functions inside the medium and its adjoint. These representations form the basis for deriving a modified version of the Marchenko method for imaging of non-reciprocal media. We illustrate the proposed method at the hand of the numerically modeled reflection response of a horizontally layered medium.

The appendices contain a detailed derivation of the unified wave equation for non-reciprocal media and the decomposition of the reciprocity theorems.

1 INTRODUCTION

Acoustic imaging methods are traditionally based on the single-scattering assumption (Claerbout 1971; Stolt 1978; Berkhout & van Wulfften Palthe 1979; Williams & Maynard 1980; Devaney 1982; Bleistein & Cohen 1982; Maynard et al. 1985; Langenberg et al. 1986; McMechan

1983; Esmersoy & Oristaglio 1988; Oristaglio 1989; Norton 1992; Wu 2004; Lindsey & Braun 2004; Etgen et al. 2009). Multiply scattered waves are not properly handled by these methods and may lead to false images overlaying the desired primary image. Several approaches have been developed that account for multiple scattering. For the sake of the discussion it is important to distinguish between different classes of multiply scattered waves. Waves that have scattered at least once at the surface of the medium are called surface-related multiples. This type of multiple scattering is particularly severe in exploration geophysics. However, because the scattering boundary is known, this class of multiples is relatively easily dealt with. Successful methods have been developed to suppress surface-related multiples prior to imaging (Verschuur et al. 1992; Carvalho et al. 1992; van Borselen et al. 1996; Biersteker 2001; Pica et al. 2005; Dragoset et al. 2010). Waves that scatter several times inside the medium before being recorded at the surface are called internal multiples. Internal multiple scattering may occur at heterogeneities at many scales. We may distinguish between deterministic scattering at well-separated scatterers, giving rise to long period multiples, and diffuse scattering in stochastic media. Of course this distinction is not always sharp. In this paper we only consider the first type of internal multiple scattering, which typically occurs in layered media (which, in general, may have curved interfaces and varying parameters in the layers). Several imaging approaches that account for deterministic internal multiples are currently under development, such as the inverse scattering series approach (Weglein et al. 1997; Ten Kroode 2002; Weglein et al. 2003), full wavefield migration (Berkhout 2014; Davydenko & Verschuur 2017), and Marchenko imaging. The latter approach builds on a 1D autofocusing procedure (Rose 2001, 2002; Broggini & Snieder 2012), which has been generalised for 2D and 3D inhomogeneous media (Wapenaar et al. 2012, 2014; Broggini et al. 2014; Behura et al. 2014; Meles et al. 2015; van der Neut et al. 2015; van der Neut & Wapenaar 2016; Thorbecke et al. 2017; Van der Neut et al. 2017; Singh et al. 2017; Mildner et al. 2017; Elison et al. 2018). This methodology predicts the internal multiples in a data-driven way and suppresses their contribution to the final image. Promising results have been obtained with geophysical (Ravasi et al. 2016; Ravasi 2017; Staring et al. 2018) and ultrasonic data (Wapenaar et al. 2018).

To date, the application of Marchenko imaging has been restricted to reciprocal media. With the increasing interest in non-reciprocal materials, both in electromagnetics (Willis 2011; He et al. 2011; Ardakani 2014) and in acoustics (Willis 2012; Norris et al. 2012; Nassar et al. 2017; Attarzadeh & Nouh 2018), it is opportune to modify the Marchenko method for imaging of non-reciprocal media. We start with a brief review of the wave equation for non-reciprocal media. By restricting this to scalar waves in a 2D plane, it is possible to capture different

wave phenomena by a unified wave equation. Next, we formulate reciprocity theorems for waves in a non-reciprocal medium and its adjoint. From these reciprocity theorems we derive Green's function representations, which form the basis for the Marchenko method in non-reciprocal media. We illustrate the new method with a numerical example, showing that it has the potential to accurately image a non-reciprocal medium, without false images related to multiple scattered waves.

2 UNIFIED WAVE EQUATION FOR NON-RECIPROCAL MEDIA

Consider the following unified equations for 2D wave propagation in the (x_1, x_3) -plane in inhomogeneous, lossless, anisotropic, non-reciprocal media

$$\alpha \partial_t P + (\partial_r + \gamma_r \partial_t) Q_r = B, \quad (1)$$

$$(\partial_r + \gamma_r \partial_t) P + \beta_{rs} \partial_t Q_s = C_r. \quad (2)$$

These equations hold for transverse-electric (TE), transverse-magnetic (TM), horizontally polarised shear (SH) and acoustic (AC) waves. They are formulated in the space-time (\mathbf{x}, t) domain, with $\mathbf{x} = (x_1, x_3)$. Operator ∂_r stands for differentiation in the x_r direction. Lower-case subscripts r and s take the values 1 and 3 only; Einstein's summation convention applies for repeated subscripts. Operator ∂_t stands for temporal differentiation. The macroscopic wave field quantities ($P = P(\mathbf{x}, t)$ and $Q_r = Q_r(\mathbf{x}, t)$), the effective medium parameters ($\alpha = \alpha(\mathbf{x})$, $\beta_{rs} = \beta_{rs}(\mathbf{x})$ and $\gamma_r = \gamma_r(\mathbf{x})$) and the macroscopic source functions ($B = B(\mathbf{x}, t)$ and $C_r = C_r(\mathbf{x}, t)$) are specified for the different wave phenomena in Table 1 (note that $\beta_{13} = \beta_{31}$). For details we refer to Appendix A.

Table 1: Quantities in unified equations (1) and (2).

	P	Q_1	Q_3	α	β_{11}	β_{31}	β_{33}	γ_1	γ_3	B	C_1	C_3
TE	E_2	H_3	$-H_1$	ε_{22}^o	μ_{33}	$-\mu_{31}$	μ_{11}	ξ_{23}	$-\xi_{21}$	$-J_2^e$	$-J_3^m$	J_1^m
TM	H_2	$-E_3$	E_1	μ_{22}	ε_{33}^o	$-\varepsilon_{31}^o$	ε_{11}^o	$-\xi_{32}$	ξ_{12}	$-J_2^m$	J_3^e	$-J_1^e$
SH	v_2	$-\tau_{21}$	$-\tau_{23}$	ρ_{22}^o	$4s_{1221}$	$4s_{1223}$	$4s_{3223}$	$2\xi_{221}$	$2\xi_{223}$	F_2	$2h_{12}$	$2h_{32}$
AC	σ	v_1	v_3	κ	ρ_{11}^o	ρ_{31}^o	ρ_{33}^o	ξ_1	ξ_3	q	F_1	F_3

By eliminating Q_r from equations (1) and (2) we obtain a scalar wave equation for field quantity P , according to

$$(\partial_r + \gamma_r \partial_t) \vartheta_{rs} (\partial_s + \gamma_s \partial_t) P - \alpha \partial_t^2 P = (\partial_r + \gamma_r \partial_t) \vartheta_{rs} C_s - \partial_t B, \quad (3)$$

see Appendix A for the derivation. Here ϑ_{rs} is the inverse of β_{rs} . Compare equation (3) with the common wave equation for waves in isotropic reciprocal media

$$\partial_r \frac{1}{\beta} \partial_r P - \alpha \partial_t^2 P = \partial_r \frac{1}{\beta} C_r - \partial_t B. \quad (4)$$

In equation (3), $\partial_r + \gamma_r \partial_t$ replaces ∂_r , with γ_r being responsible for the non-reciprocal behaviour. Moreover, ϑ_{rs} replaces $1/\beta$, thus accounting for anisotropy of the effective non-reciprocal medium.

3 RECIPROCITY THEOREMS FOR A NON-RECIPROCAL MEDIUM AND ITS ADJOINT

We derive reciprocity theorems in the space-frequency (\mathbf{x}, ω) -domain for wave fields in a non-reciprocal medium and its adjoint. To this end, we define the temporal Fourier transform of a space- and time-dependent function $f(\mathbf{x}, t)$ as

$$f(\mathbf{x}, \omega) = \int_{-\infty}^{\infty} \exp(i\omega t) f(\mathbf{x}, t) dt, \quad (5)$$

where ω is the angular frequency and i the imaginary unit. For notational convenience we use the same symbol for quantities in the time domain and in the frequency domain. We use equation (5) to transform equations (1) and (2) to the space-frequency domain. The temporal differential operators ∂_t are thus replaced by $-i\omega$, hence

$$-i\omega \alpha P + (\partial_r - i\omega \gamma_r) Q_r = B, \quad (6)$$

$$(\partial_r - i\omega \gamma_r) P - i\omega \beta_{rs} Q_s = C_r, \quad (7)$$

with $P = P(\mathbf{x}, \omega)$, $Q_r = Q_r(\mathbf{x}, \omega)$, $B = B(\mathbf{x}, \omega)$ and $C_r = C_r(\mathbf{x}, \omega)$. A reciprocity theorem formulates a mathematical relation between two independent states (Fokkema & van den Berg 1993; de Hoop 1995; Achenbach 2003). We indicate the sources, medium parameters and wave fields in the two states by subscripts A and B . Consider the quantity

$$\partial_r (P_A Q_{r,B} - Q_{r,A} P_B). \quad (8)$$

Applying the product rule for differentiation, using equations (6) and (7) for states A and B , using $\beta_{sr} = \beta_{rs}$, integrating the result over domain \mathbb{D} enclosed by boundary $\partial\mathbb{D}$ with outward

pointing normal vector $\mathbf{n} = (n_1, n_3)$ and applying the theorem of Gauss, we obtain

$$\begin{aligned}
 \oint_{\partial\mathbb{D}} (P_A Q_{r,B} - Q_{r,A} P_B) n_r d\mathbf{x} = & \quad (9) \\
 i\omega \int_{\mathbb{D}} \left((\alpha_B - \alpha_A) P_A P_B - (\beta_{rs,B} - \beta_{rs,A}) Q_{r,A} Q_{s,B} \right) d\mathbf{x} \\
 + i\omega \int_{\mathbb{D}} (\gamma_{r,B} + \gamma_{r,A}) (P_A Q_{r,B} - Q_{r,A} P_B) d\mathbf{x} \\
 + \int_{\mathbb{D}} (C_{r,A} Q_{r,B} - Q_{r,A} C_{r,B} + P_A B_B - B_A P_B) d\mathbf{x}.
 \end{aligned}$$

This is the general reciprocity theorem of the convolution type. When the medium parameters α , β_{rs} and γ_r are identical in both states, then the first integral on the right-hand side vanishes, but the second integral, containing γ_r , does not vanish. This confirms that γ_r is the parameter responsible for the non-reciprocal behaviour. When we choose $\gamma_{r,A} = -\gamma_{r,B} = -\gamma_r$, then the second integral also vanishes. For this situation we call state B , with parameters α , β_{rs} and γ_r , the actual state, and state A , with parameters α , β_{rs} and $-\gamma_r$, the adjoint state. We indicate the adjoint state by a superscript (a) . Hence

$$\begin{aligned}
 \oint_{\partial\mathbb{D}} (P_A^{(a)} Q_{r,B} - Q_{r,A}^{(a)} P_B) n_r d\mathbf{x} = & \quad (10) \\
 \int_{\mathbb{D}} (C_{r,A}^{(a)} Q_{r,B} - Q_{r,A}^{(a)} C_{r,B} + P_A^{(a)} B_B - B_A^{(a)} P_B) d\mathbf{x}.
 \end{aligned}$$

This reciprocity theorem will play a role in the derivation of Green's function representations for the Marchenko method for non-reciprocal media (section 4). Here we use it to derive a relation between Green's functions in states A and B . For the adjoint state A we choose a unit monopole point source at \mathbf{x}_S in \mathbb{D} , hence $B_A^{(a)}(\mathbf{x}, \omega) = \delta(\mathbf{x} - \mathbf{x}_S)$, where $\delta(\mathbf{x})$ is the Dirac delta function. The response to this point source is the Green's function in state A , hence $P_A^{(a)}(\mathbf{x}, \omega) = G^{(a)}(\mathbf{x}, \mathbf{x}_S, \omega)$. Similarly, for state B we choose a unit monopole point source at \mathbf{x}_R in \mathbb{D} , hence $B_B(\mathbf{x}, \omega) = \delta(\mathbf{x} - \mathbf{x}_R)$ and $P_B(\mathbf{x}, \omega) = G(\mathbf{x}, \mathbf{x}_R, \omega)$. We substitute these expressions into equation (10) and set the other source quantities, $C_{r,A}^{(a)}$ and $C_{r,B}$, to zero. Further, we assume that Neumann or Dirichlet boundary conditions apply at $\partial\mathbb{D}$, or that the medium at and outside $\partial\mathbb{D}$ is homogeneous and reciprocal. In each of these cases the boundary integral vanishes. We thus obtain (Slob & Wapenaar 2009; Willis 2012)

$$G^{(a)}(\mathbf{x}_R, \mathbf{x}_S, \omega) = G(\mathbf{x}_S, \mathbf{x}_R, \omega). \quad (11)$$

The left-hand side is the response to a source at \mathbf{x}_S in the adjoint medium (with parameter $-\gamma_r$), observed by a receiver at \mathbf{x}_R . The right-hand side is the response to a source at \mathbf{x}_R in the actual medium (with parameter γ_r), observed by a receiver at \mathbf{x}_S . Note the analogy with

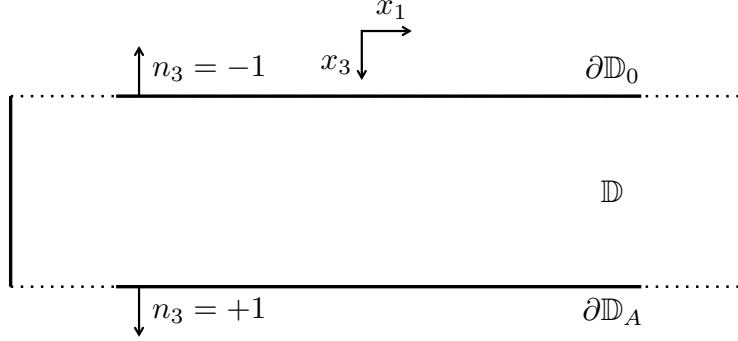


Figure 1. Modified configuration for the reciprocity theorems.

the flow-reversal theorem for waves in flowing media (Lyamshev 1961; Godin 1997; Wapenaar & Fokkema 2004).

Next, we consider the quantity

$$\partial_r(P_A^*Q_{r,B} + Q_{r,A}^*P_B). \quad (12)$$

Superscript * denotes complex conjugation. Following the same steps as before, we obtain

$$\begin{aligned} \oint_{\partial\mathbb{D}} (P_A^*Q_{r,B} + Q_{r,A}^*P_B)n_r d\mathbf{x} = & \quad (13) \\ i\omega \int_{\mathbb{D}} \left((\alpha_B - \alpha_A)P_A^*P_B + (\beta_{rs,B} - \beta_{rs,A})Q_{r,A}^*Q_{s,B} \right) d\mathbf{x} \\ + \int_{\mathbb{D}} i\omega(\gamma_{r,B} - \gamma_{r,A})(P_A^*Q_{r,B} + Q_{r,A}^*P_B) d\mathbf{x} \\ + \int_{\mathbb{D}} (C_{r,A}^*Q_{r,B} + Q_{r,A}^*C_{r,B} + P_A^*B_B + B_A^*P_B) d\mathbf{x}. \end{aligned}$$

This is the general reciprocity theorem of the correlation type. When the medium parameters α , β_{rs} and γ_r are identical in both states, then the first and second integral on the right-hand side vanish. Hence

$$\begin{aligned} \oint_{\partial\mathbb{D}} (P_A^*Q_{r,B} + Q_{r,A}^*P_B)n_r d\mathbf{x} = & \quad (14) \\ \int_{\mathbb{D}} (C_{r,A}^*Q_{r,B} + Q_{r,A}^*C_{r,B} + P_A^*B_B + B_A^*P_B) d\mathbf{x}. \end{aligned}$$

Also this reciprocity theorem will play a role in the derivation of Green's function representations for the Marchenko method for non-reciprocal media.

4 GREEN'S FUNCTION REPRESENTATIONS FOR THE MARCHENKO METHOD

We use the reciprocity theorems of the convolution and correlation type (equations (10) and (14)) to derive Green's function representations for the Marchenko method for non-reciprocal media. The derivation is similar to that for reciprocal media (Wapenaar et al. 2014); here we emphasise the differences. We consider a spatial domain \mathbb{D} , enclosed by two infinite horizontal boundaries $\partial\mathbb{D}_0$ and $\partial\mathbb{D}_A$ (with $\partial\mathbb{D}_A$ below $\partial\mathbb{D}_0$), and two finite vertical side boundaries (at $x_1 \rightarrow \pm\infty$), see Figure 1. The positive x_3 -axis points downward. The normal vectors at $\partial\mathbb{D}_0$ and $\partial\mathbb{D}_A$ are $\mathbf{n} = (0, -1)$ and $\mathbf{n} = (0, 1)$, respectively. The boundary integrals in equations (10) and (14) along the vertical side boundaries vanish (Wapenaar & Berkhout 1989). Assuming there are no sources in \mathbb{D} in both states, the reciprocity theorems thus simplify to

$$\int_{\partial\mathbb{D}_0} (P_A^{(a)} Q_{3,B} - Q_{3,A}^{(a)} P_B) dx_1 = \int_{\partial\mathbb{D}_A} (P_A^{(a)} Q_{3,B} - Q_{3,A}^{(a)} P_B) dx_1 \quad (15)$$

and

$$\int_{\partial\mathbb{D}_0} (P_A^* Q_{3,B} + Q_{3,A}^* P_B) dx_1 = \int_{\partial\mathbb{D}_A} (P_A^* Q_{3,B} + Q_{3,A}^* P_B) dx_1. \quad (16)$$

For the derivation of the representations for the Marchenko method it is convenient to decompose the wave field quantities in these theorems into downgoing and upgoing fields in both states. Consider the following relations

$$\mathbf{q} = \mathcal{L}\mathbf{p}, \quad \mathbf{p} = \mathcal{L}^{-1}\mathbf{q}, \quad (17)$$

with wave vectors $\mathbf{q} = \mathbf{q}(\mathbf{x}, \omega)$ and $\mathbf{p} = \mathbf{p}(\mathbf{x}, \omega)$ defined as

$$\mathbf{q} = \begin{pmatrix} P \\ Q_3 \end{pmatrix}, \quad \mathbf{p} = \begin{pmatrix} U^+ \\ U^- \end{pmatrix}. \quad (18)$$

Here $U^+ = U^+(\mathbf{x}, \omega)$ and $U^- = U^-(\mathbf{x}, \omega)$ are downgoing and upgoing wave fields, respectively. Operator $\mathcal{L} = \mathcal{L}(\mathbf{x}, \omega)$ in equation (17) is a pseudo-differential operator that composes the total wave field from its downgoing and upgoing constituents (Corones et al. 1983; Fishman et al. 1987; Wapenaar & Berkhout 1989; Fishman 1993; de Hoop 1992; de Hoop 1996; Wapenaar 1996; Haines & de Hoop 1996; Fishman et al. 2000). Its inverse decomposes the total wave field into downgoing and upgoing fields. For inhomogeneous isotropic reciprocal media, the theory for this operator is well developed. For anisotropic non-reciprocal media we restrict the application of this operator to the laterally invariant situation. In Appendix B we use equations (17) and (18) at boundaries $\partial\mathbb{D}_0$ and $\partial\mathbb{D}_A$ to recast reciprocity theorems (15)

and (16) as follows

$$\int_{\partial\mathbb{D}_0} (U_A^{+(a)}U_B^- - U_A^{-(a)}U_B^+)dx_1 = \int_{\partial\mathbb{D}_A} (U_A^{+(a)}U_B^- - U_A^{-(a)}U_B^+)dx_1 \quad (19)$$

and

$$\int_{\partial\mathbb{D}_0} (U_A^{+*}U_B^+ - U_A^{-*}U_B^-)dx_1 = \int_{\partial\mathbb{D}_A} (U_A^{+*}U_B^+ - U_A^{-*}U_B^-)dx_1. \quad (20)$$

Note that the assumption of lateral invariance only applies to boundaries $\partial\mathbb{D}_0$ and $\partial\mathbb{D}_A$; the remainder of the medium (in- and outside \mathbb{D}) may be arbitrary inhomogeneous. Equation (19) is exact, whereas in equation (20) evanescent waves are neglected at boundaries $\partial\mathbb{D}_0$ and $\partial\mathbb{D}_A$.

Table 2: Quantities to derive equations (22) and (23).

	$U_A^+(\mathbf{x}, \omega)$	$U_A^-(\mathbf{x}, \omega)$	$U_B^+(\mathbf{x}, \omega)$	$U_B^-(\mathbf{x}, \omega)$
$\mathbf{x} = (x_1, x_{3,0})$ at $\partial\mathbb{D}_0$	$f_1^+(\mathbf{x}, \mathbf{x}_A, \omega)$	$f_1^-(\mathbf{x}, \mathbf{x}_A, \omega)$	$\delta(x_1 - x_{1,S})$	$R(\mathbf{x}, \mathbf{x}_S, \omega)$
$\mathbf{x} = (x_1, x_{3,A})$ at $\partial\mathbb{D}_A$	$\delta(x_1 - x_{1,A})$	0	$G^+(\mathbf{x}, \mathbf{x}_S, \omega)$	$G^-(\mathbf{x}, \mathbf{x}_S, \omega)$

In the following we define $\partial\mathbb{D}_0$ (at $x_3 = x_{3,0}$) as the upper boundary of an inhomogeneous, anisotropic, non-reciprocal, lossless medium. Furthermore, we define $\partial\mathbb{D}_A$ (at $x_3 = x_{3,A}$, with $x_{3,A} > x_{3,0}$) as an arbitrary boundary inside the medium. We assume that the medium above $\partial\mathbb{D}_0$ is homogeneous. For state *B* we consider a unit source for downgoing waves at $\mathbf{x}_S = (x_{1,S}, x_{3,S})$, just above $\partial\mathbb{D}_0$ (hence, $x_{3,S} = x_{3,0} - \epsilon$, with $\epsilon \rightarrow 0$). The response to this unit source at any observation point \mathbf{x} is given by $U_B^\pm(\mathbf{x}, \omega) = G^\pm(\mathbf{x}, \mathbf{x}_S, \omega)$, where G^+ and G^- denote the downgoing and upgoing components of the Green's function. For \mathbf{x} at $\partial\mathbb{D}_0$, i.e., just below the source, we have $U_B^+(\mathbf{x}, \omega) = G^+(\mathbf{x}, \mathbf{x}_S, \omega) = \delta(x_1 - x_{1,S})$ and $U_B^-(\mathbf{x}, \omega) = G^-(\mathbf{x}, \mathbf{x}_S, \omega) = R(\mathbf{x}, \mathbf{x}_S, \omega)$, with $R(\mathbf{x}, \mathbf{x}_S, \omega)$ denoting the reflection response at $\partial\mathbb{D}_0$ of the medium below $\partial\mathbb{D}_0$. At $\partial\mathbb{D}_A$, we have $U_B^\pm(\mathbf{x}, \omega) = G^\pm(\mathbf{x}, \mathbf{x}_S, \omega)$. For state *A* we consider a focal point at $\mathbf{x}_A = (x_{1,A}, x_{3,A})$ at $\partial\mathbb{D}_A$. The medium in state *A* is a truncated medium, which is identical to the actual medium between $\partial\mathbb{D}_0$ and $\partial\mathbb{D}_A$, and homogeneous below $\partial\mathbb{D}_A$. At $\partial\mathbb{D}_0$ a downgoing focusing function $U_A^+(\mathbf{x}, \omega) = f_1^+(\mathbf{x}, \mathbf{x}_A, \omega)$, with $\mathbf{x} = (x_1, x_{3,0})$, is incident to the truncated medium. This function focuses at \mathbf{x}_A , hence, at $\partial\mathbb{D}_A$ we have $U_A^+(\mathbf{x}, \omega) = f_1^+(\mathbf{x}, \mathbf{x}_A, \omega) = \delta(x_1 - x_{1,A})$. The response to this focusing function at $\partial\mathbb{D}_0$ is $U_A^-(\mathbf{x}, \omega) = f_1^-(\mathbf{x}, \mathbf{x}_A, \omega)$. Because the truncated medium is homogeneous below $\partial\mathbb{D}_A$, we have $U_A^-(\mathbf{x}, \omega) = 0$ at $\partial\mathbb{D}_A$. The quantities for both states are summarised in Table 2.

Note that the downgoing focusing function $f_1^+(\mathbf{x}, \mathbf{x}_A, \omega)$, for \mathbf{x} at $\partial\mathbb{D}_0$, is the inverse of the

transmission response $T(\mathbf{x}_A, \mathbf{x}, \omega)$ of the truncated medium (Wapenaar et al. 2014), hence

$$f_1^+(\mathbf{x}, \mathbf{x}_A, \omega) = T^{\text{inv}}(\mathbf{x}_A, \mathbf{x}, \omega), \quad (21)$$

for \mathbf{x} at $\partial\mathbb{D}_0$. To avoid instabilities in the evanescent field, the focusing function is in practice spatially band-limited.

Substituting the quantities of Table 2 into equations (19) and (20) gives

$$G^-(\mathbf{x}_A, \mathbf{x}_S, \omega) + f_1^{-(a)}(\mathbf{x}_S, \mathbf{x}_A, \omega) = \int_{\partial\mathbb{D}_0} R(\mathbf{x}, \mathbf{x}_S, \omega) f_1^{+(a)}(\mathbf{x}, \mathbf{x}_A, \omega) dx_1 \quad (22)$$

and

$$G^+(\mathbf{x}_A, \mathbf{x}_S, \omega) - \{f_1^+(\mathbf{x}_S, \mathbf{x}_A, \omega)\}^* = - \int_{\partial\mathbb{D}_0} R(\mathbf{x}, \mathbf{x}_S, \omega) \{f_1^-(\mathbf{x}, \mathbf{x}_A, \omega)\}^* dx_1, \quad (23)$$

respectively. These are two representations for the upgoing and downgoing parts of the Green's function between \mathbf{x}_S at the acquisition surface and \mathbf{x}_A inside the non-reciprocal medium.

They are expressed in terms of the reflection response $R(\mathbf{x}, \mathbf{x}_S, \omega)$ and a number of focusing functions. Unlike similar representations for reciprocal media (Slob et al. 2014; Wapenaar et al. 2014), the focusing functions in equation (22) are defined in the adjoint of the truncated medium. Therefore we cannot use the standard approach to retrieve the focusing functions and Green's functions from the reflection response $R(\mathbf{x}, \mathbf{x}_S, \omega)$. We obtain a second set of representations by replacing all quantities in equations (22) and (23) by the corresponding quantities in the adjoint medium. For the focusing functions in equation (22) this implies they are replaced by their counterparts in the truncated actual medium. We thus obtain

$$G^{-(a)}(\mathbf{x}_A, \mathbf{x}_S, \omega) + f_1^{-(a)}(\mathbf{x}_S, \mathbf{x}_A, \omega) = \int_{\partial\mathbb{D}_0} R^{(a)}(\mathbf{x}, \mathbf{x}_S, \omega) f_1^+(\mathbf{x}, \mathbf{x}_A, \omega) dx_1 \quad (24)$$

and

$$G^{+(a)}(\mathbf{x}_A, \mathbf{x}_S, \omega) - \{f_1^{+(a)}(\mathbf{x}_S, \mathbf{x}_A, \omega)\}^* = - \int_{\partial\mathbb{D}_0} R^{(a)}(\mathbf{x}, \mathbf{x}_S, \omega) \{f_1^{-(a)}(\mathbf{x}, \mathbf{x}_A, \omega)\}^* dx_1 \quad (25)$$

respectively. Because in practical situations we do not have access to the reflection response $R^{(a)}(\mathbf{x}, \mathbf{x}_S, \omega)$ in the adjoint medium, we derive a relation analogous to equation (11) for this reflection response. To this end, consider the quantities in Table 3, with \mathbf{x}_S and \mathbf{x}_R just above $\partial\mathbb{D}_0$, and with $\partial\mathbb{D}_M$ denoting a boundary below all inhomogeneities, so that there are no upgoing waves at $\partial\mathbb{D}_M$. Substituting the quantities of Table 3 into equation (19) (with $\partial\mathbb{D}_A$ replaced by $\partial\mathbb{D}_M$) gives

$$R^{(a)}(\mathbf{x}_R, \mathbf{x}_S, \omega) = R(\mathbf{x}_S, \mathbf{x}_R, \omega). \quad (26)$$

Equations (22) – (25), with $R^{(a)}(\mathbf{x}, \mathbf{x}_S, \omega)$ replaced by $R(\mathbf{x}_S, \mathbf{x}, \omega)$, form the basis for the Marchenko method, discussed in the next section.

Table 3: Quantities to derive equation (26).

	$U_A^{+(a)}(\mathbf{x}, \omega)$	$U_A^{- (a)}(\mathbf{x}, \omega)$	$U_B^+(\mathbf{x}, \omega)$	$U_B^-(\mathbf{x}, \omega)$
$\mathbf{x} = (x_1, x_{3,0})$ at $\partial\mathbb{D}_0$	$\delta(x_1 - x_{1,S})$	$R^{(a)}(\mathbf{x}, \mathbf{x}_S, \omega)$	$\delta(x_1 - x_{1,R})$	$R(\mathbf{x}, \mathbf{x}_R, \omega)$
$\mathbf{x} = (x_1, x_{3,M})$ at $\partial\mathbb{D}_M$	$G^{+(a)}(\mathbf{x}, \mathbf{x}_S, \omega)$	0	$G^+(\mathbf{x}, \mathbf{x}_R, \omega)$	0

5 THE MARCHENKO METHOD FOR NON-RECIPROCAL MEDIA

The standard multidimensional Marchenko method for reciprocal media (Slob et al. 2014; Wapenaar et al. 2014) uses the representations of equations (22) and (23), but without the superscript (a) , to retrieve the focusing functions from the reflection response. Here we discuss how to modify this method for non-reciprocal media. We separate the representations of equations (22) – (25) into two sets, each set containing focusing functions in one and the same truncated medium. These sets are equations (23) and (24), with the focusing functions in the truncated actual medium, and equations (22) and (25), with the focusing functions in the truncated adjoint medium. We start with the set of equations (23) and (24), which read in the time domain (using equation (26))

$$G^+(\mathbf{x}_A, \mathbf{x}_S, t) - f_1^+(\mathbf{x}_S, \mathbf{x}_A, -t) = - \int_{\partial\mathbb{D}_0} dx_1 \int_{-\infty}^t R(\mathbf{x}, \mathbf{x}_S, t - t') f_1^-(\mathbf{x}, \mathbf{x}_A, -t') dt' \quad (27)$$

and

$$G^{-(a)}(\mathbf{x}_A, \mathbf{x}_S, t) + f_1^-(\mathbf{x}_S, \mathbf{x}_A, t) = \int_{\partial\mathbb{D}_0} dx_1 \int_{-\infty}^t R(\mathbf{x}_S, \mathbf{x}, t - t') f_1^+(\mathbf{x}, \mathbf{x}_A, t') dt', \quad (28)$$

respectively. We introduce time windows to remove the Green's functions from these representations. Similar as in the reciprocal situation, we assume that the Green's function and the time-reversed focusing function on the left-hand side of equation (27) are separated in time, except for the direct arrivals (Wapenaar et al. 2014). This is a reasonable assumption for media with smooth lateral variations, and for limited horizontal source-receiver distances. Let $t_d(\mathbf{x}_A, \mathbf{x}_S)$ denote the travel time of the direct arrival of $G^+(\mathbf{x}_A, \mathbf{x}_S, t)$. We define a time window $w(\mathbf{x}_A, \mathbf{x}_S, t) = u(t_d(\mathbf{x}_A, \mathbf{x}_S) - t_\epsilon - t)$, where $u(t)$ is the Heaviside function and t_ϵ a small positive time constant. Under the above-mentioned assumption, we have $w(\mathbf{x}_A, \mathbf{x}_S, t)G^+(\mathbf{x}_A, \mathbf{x}_S, t) = 0$. For the focusing function on the left-hand side of equation (27) we write (Wapenaar et al. 2014)

$$\begin{aligned} f_1^+(\mathbf{x}_S, \mathbf{x}_A, t) &= T^{\text{inv}}(\mathbf{x}_A, \mathbf{x}_S, \omega) \\ &= T_d^{\text{inv}}(\mathbf{x}_A, \mathbf{x}_S, t) + M^+(\mathbf{x}_S, \mathbf{x}_A, t), \end{aligned} \quad (29)$$

where $T_d^{\text{inv}}(\mathbf{x}_A, \mathbf{x}_S, t)$ is the inverse of the direct arrival of the transmission response of the truncated medium and $M^+(\mathbf{x}_S, \mathbf{x}_A, t)$ the scattering coda. The travel time of $T_d^{\text{inv}}(\mathbf{x}_A, \mathbf{x}_S, t)$ is $-t_d(\mathbf{x}_A, \mathbf{x}_S)$ and the scattering coda obeys $M^+(\mathbf{x}_S, \mathbf{x}_A, t) = 0$ for $t \leq -t_d(\mathbf{x}_A, \mathbf{x}_S)$. Hence, $w(\mathbf{x}_A, \mathbf{x}_S, t)f_1^+(\mathbf{x}_S, \mathbf{x}_A, -t) = M^+(\mathbf{x}_S, \mathbf{x}_A, -t)$. Applying the time window $w(\mathbf{x}_A, \mathbf{x}_S, t)$ to both sides of equation (27) thus yields

$$M^+(\mathbf{x}_S, \mathbf{x}_A, -t) = w(\mathbf{x}_A, \mathbf{x}_S, t) \int_{\partial\mathbb{D}_0} dx_1 \int_{-\infty}^t R(\mathbf{x}, \mathbf{x}_S, t-t') f_1^-(\mathbf{x}, \mathbf{x}_A, -t') dt'. \quad (30)$$

We assume that the Green's function and the focusing function in the left-hand side of equation (28) are separated in time (without overlap). Unlike for reciprocal media, we need a different time window to suppress the Green's function, because the latter is defined in the adjoint medium. To this end we define a time window $w^{(a)}(\mathbf{x}_A, \mathbf{x}_S, t) = u(t_d^{(a)}(\mathbf{x}_A, \mathbf{x}_S) - t_\epsilon - t)$, where $t_d^{(a)}(\mathbf{x}_A, \mathbf{x}_S)$ denotes the travel time of the direct arrival in the adjoint medium. Applying this window to both sides of equation (28) yields

$$f_1^-(\mathbf{x}_S, \mathbf{x}_A, t) = w^{(a)}(\mathbf{x}_A, \mathbf{x}_S, t) \int_{\partial\mathbb{D}_0} dx_1 \int_{-\infty}^t R(\mathbf{x}_S, \mathbf{x}, t-t') f_1^+(\mathbf{x}, \mathbf{x}_A, t') dt'. \quad (31)$$

Equations (30) and (31), with f_1^+ given by equation (29), form a set of two equations for the two unknown functions $M^+(\mathbf{x}, \mathbf{x}_A, t)$ and $f_1^-(\mathbf{x}, \mathbf{x}_A, t)$ (with \mathbf{x} at $\partial\mathbb{D}_0$). These functions can be resolved from equations (30) and (31), assuming $R(\mathbf{x}, \mathbf{x}_S, t)$, $R(\mathbf{x}_S, \mathbf{x}, t)$, $t_d(\mathbf{x}_A, \mathbf{x}_S)$, $t_d^{(a)}(\mathbf{x}_A, \mathbf{x}_S)$ and $T_d^{\text{inv}}(\mathbf{x}_A, \mathbf{x}_S, t)$ are known for all \mathbf{x} and \mathbf{x}_S at $\partial\mathbb{D}_0$. The reflection responses $R(\mathbf{x}, \mathbf{x}_S, t)$ and $R(\mathbf{x}_S, \mathbf{x}, t)$ are obtained from measurements at the upper boundary $\partial\mathbb{D}_0$ of the medium. This involves deconvolution for the source function, decomposition and, when the upper boundary is a reflecting boundary, elimination of the surface-related multiple reflections (Verschuur et al. 1992). The travel times $t_d(\mathbf{x}_A, \mathbf{x}_S)$ and $t_d^{(a)}(\mathbf{x}_A, \mathbf{x}_S)$, and the inverse of the direct arrival of the transmission response, $T_d^{\text{inv}}(\mathbf{x}_A, \mathbf{x}_S, t)$, can be derived from a background model of the medium and its adjoint. A smooth background model is sufficient to derive these quantities, hence, no information about the scattering interfaces inside the medium is required. The iterative Marchenko scheme to solve for $M^+(\mathbf{x}, \mathbf{x}_A, t)$ and $f_1^-(\mathbf{x}, \mathbf{x}_A, t)$ reads

$$f_{1,k}^-(\mathbf{x}_S, \mathbf{x}_A, t) = w^{(a)}(\mathbf{x}_A, \mathbf{x}_S, t) \int_{\partial\mathbb{D}_0} dx_1 \int_{-\infty}^t R(\mathbf{x}_S, \mathbf{x}, t-t') f_{1,k}^+(\mathbf{x}, \mathbf{x}_A, t') dt', \quad (32)$$

$$M_{k+1}^+(\mathbf{x}_S, \mathbf{x}_A, -t) = w(\mathbf{x}_A, \mathbf{x}_S, t) \int_{\partial\mathbb{D}_0} dx_1 \int_{-\infty}^t R(\mathbf{x}, \mathbf{x}_S, t-t') f_{1,k}^-(\mathbf{x}, \mathbf{x}_A, -t') dt', \quad (33)$$

with

$$f_{1,k}^+(\mathbf{x}, \mathbf{x}_A, t) = T_d^{\text{inv}}(\mathbf{x}_A, \mathbf{x}, t) + M_k^+(\mathbf{x}, \mathbf{x}_A, t), \quad (34)$$

starting with $M_0^+(\mathbf{x}, \mathbf{x}_A, t) = 0$. Once $M^+(\mathbf{x}, \mathbf{x}_A, t)$ and $f_1^-(\mathbf{x}, \mathbf{x}_A, t)$ are found, $f_1^+(\mathbf{x}, \mathbf{x}_A, t)$ is obtained from equation (29) and, subsequently, the Green's functions $G^+(\mathbf{x}_A, \mathbf{x}_S, t)$ and

$G^{-(a)}(\mathbf{x}_A, \mathbf{x}_S, t)$ are obtained from equations (27) and (28). Note that only $G^+(\mathbf{x}_A, \mathbf{x}_S, t)$ is defined in the actual medium. To obtain $G^-(\mathbf{x}_A, \mathbf{x}_S, t)$ in the actual medium we consider the set of equations (22) and (25), which read in the time domain (using equation (26))

$$G^-(\mathbf{x}_A, \mathbf{x}_S, t) + f_1^{-(a)}(\mathbf{x}_S, \mathbf{x}_A, t) = \int_{\partial\mathbb{D}_0} dx_1 \int_{-\infty}^t R(\mathbf{x}, \mathbf{x}_S, t-t') f_1^{+(a)}(\mathbf{x}, \mathbf{x}_A, t') dt' \quad (35)$$

and

$$G^{+(a)}(\mathbf{x}_A, \mathbf{x}_S, t) - f_1^{+(a)}(\mathbf{x}_S, \mathbf{x}_A, -t) = - \int_{\partial\mathbb{D}_0} dx_1 \int_{-\infty}^t R(\mathbf{x}_S, \mathbf{x}, t-t') f_1^{-(a)}(\mathbf{x}, \mathbf{x}_A, -t') dt', \quad (36)$$

respectively. The same reasoning as above leads to the following iterative Marchenko scheme for the focusing functions in the truncated adjoint medium

$$f_{1,k}^{-(a)}(\mathbf{x}_S, \mathbf{x}_A, t) = w(\mathbf{x}_A, \mathbf{x}_S, t) \int_{\partial\mathbb{D}_0} dx_1 \int_{-\infty}^t R(\mathbf{x}, \mathbf{x}_S, t-t') f_{1,k}^{+(a)}(\mathbf{x}, \mathbf{x}_A, t') dt' \quad (37)$$

$$M_{k+1}^{+(a)}(\mathbf{x}_S, \mathbf{x}_A, -t) = w^{(a)}(\mathbf{x}_A, \mathbf{x}_S, t) \int_{\partial\mathbb{D}_0} dx_1 \int_{-\infty}^t R(\mathbf{x}_S, \mathbf{x}, t-t') f_{1,k}^{-(a)}(\mathbf{x}, \mathbf{x}_A, -t') dt', \quad (38)$$

with

$$f_{1,k}^{+(a)}(\mathbf{x}, \mathbf{x}_A, t) = T_d^{\text{inv}(a)}(\mathbf{x}_A, \mathbf{x}, t) + M_k^{+(a)}(\mathbf{x}, \mathbf{x}_A, t), \quad (39)$$

starting with $M_0^{+(a)}(\mathbf{x}, \mathbf{x}_A, t) = 0$. Here $T_d^{\text{inv}(a)}(\mathbf{x}_A, \mathbf{x}, t)$ can be derived from the adjoint background model. Once the focusing functions $f_1^{+(a)}(\mathbf{x}, \mathbf{x}_A, t)$ and $f_1^{-(a)}(\mathbf{x}, \mathbf{x}_A, t)$ are found, the Green's functions $G^-(\mathbf{x}_A, \mathbf{x}_S, t)$ and $G^{+(a)}(\mathbf{x}_A, \mathbf{x}_S, t)$ are obtained from equations (35) and (36).

We conclude this section by showing how $G^+(\mathbf{x}_A, \mathbf{x}_S, t)$ and $G^-(\mathbf{x}_A, \mathbf{x}_S, t)$ can be used to image the interior of the non-reciprocal medium. First we derive a mutual relation between these Green's functions. To this end, consider the quantities in Table 4. Here $R^{(a)}(\mathbf{x}, \mathbf{x}_A, \omega)$ in state A is the reflection response at $\partial\mathbb{D}_A$ of the adjoint medium below $\partial\mathbb{D}_A$, with \mathbf{x}_A defined just above $\partial\mathbb{D}_A$ and the medium in state A being homogeneous above $\partial\mathbb{D}_A$. Substituting the quantities of Table 4 into equation (19) (with $\partial\mathbb{D}_0$ and $\partial\mathbb{D}_A$ replaced by $\partial\mathbb{D}_A$ and $\partial\mathbb{D}_M$, respectively) gives

$$G^-(\mathbf{x}_A, \mathbf{x}_S, \omega) = \int_{\partial\mathbb{D}_A} R^{(a)}(\mathbf{x}, \mathbf{x}_A, \omega) G^+(\mathbf{x}, \mathbf{x}_S, \omega) dx_1, \quad (40)$$

or, using equation (26) and applying an inverse Fourier transformation to the time domain,

$$G^-(\mathbf{x}_A, \mathbf{x}_S, t) = \int_{\partial\mathbb{D}_A} dx_1 \int_{-\infty}^t R(\mathbf{x}_A, \mathbf{x}, t-t') G^+(\mathbf{x}, \mathbf{x}_S, t') dt'. \quad (41)$$

Given the Green's functions $G^+(\mathbf{x}, \mathbf{x}_S, t)$ and $G^-(\mathbf{x}_A, \mathbf{x}_S, t)$ for all \mathbf{x}_A and \mathbf{x} at $\partial\mathbb{D}_A$ for a range of source positions \mathbf{x}_S at $\partial\mathbb{D}_0$, the reflection response $R(\mathbf{x}_A, \mathbf{x}, t)$ for all \mathbf{x}_A and \mathbf{x} at $\partial\mathbb{D}_A$ can be resolved by multidimensional deconvolution (Wapenaar et al. 2000; Amundsen 2001; Holvik & Amundsen 2005; Wapenaar & van der Neut 2010; van der Neut et al. 2011;

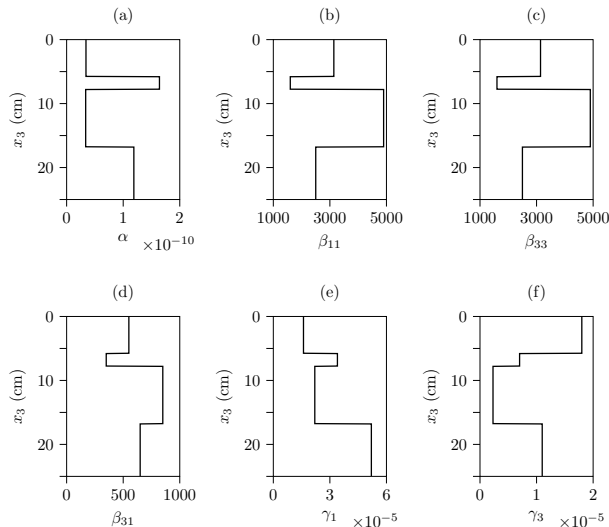


Figure 2. Parameters $\alpha(x_3)$, $\beta_{11}(x_3)$, $\beta_{33}(x_3)$, $\beta_{31}(x_3)$, $\gamma_1(x_3)$ and $\gamma_3(x_3)$ of the layered medium.

Ravasi et al. 2015). An image can be obtained by selecting $R(\mathbf{x}, \mathbf{x}, t = 0)$ and repeating the process for any \mathbf{x} in the region of interest.

Table 4: Quantities to derive equation (40).

	$U_A^{+(a)}(\mathbf{x}, \omega)$	$U_A^{- (a)}(\mathbf{x}, \omega)$	$U_B^+(\mathbf{x}, \omega)$	$U_B^-(\mathbf{x}, \omega)$
$\mathbf{x} = (x_1, x_{3,A})$ at $\partial\mathbb{D}_A$	$\delta(x_1 - x_{1,A})$	$R^{(a)}(\mathbf{x}, \mathbf{x}_A, \omega)$	$G^+(\mathbf{x}, \mathbf{x}_S, \omega)$	$G^-(\mathbf{x}, \mathbf{x}_S, \omega)$
$\mathbf{x} = (x_1, x_{3,M})$ at $\partial\mathbb{D}_M$	$G^{+(a)}(\mathbf{x}, \mathbf{x}_A, \omega)$	0	$G^+(\mathbf{x}, \mathbf{x}_S, \omega)$	0

6 NUMERICAL EXAMPLE

We illustrate the proposed methodology with a numerical example. For simplicity we consider a horizontally layered medium, consisting of three homogeneous layers and a homogeneous half-space below the deepest layer. The medium parameters of the layered medium, $\alpha(x_3)$, $\beta_{rs}(x_3)$ and $\gamma_r(x_3)$ are shown in Figure 2. In many practical situations the parameters $\beta_{31}(x_3)$ and $\gamma_3(x_3)$ will be zero, but we choose them to be non-zero to demonstrate the generality of the method. We define a source at $\mathbf{x}_S = (0, 0)$ at the top of the first layer, which emits a time-symmetric wavelet $S(t)$ with a central frequency of 600 kHz into the layered medium. We use a wavenumber-frequency domain modelling method (Kennett & Kerry 1979), adjusted for non-reciprocal media, to model the response to this source. The modelled reflection response, $R(\mathbf{x}, \mathbf{x}_S, t) * S(t)$ at $\partial\mathbb{D}_0$ (the asterisk denoting convolution), is shown in Figure 3. To emphasise the multiple scattering, a time-dependent amplitude gain has been applied, using

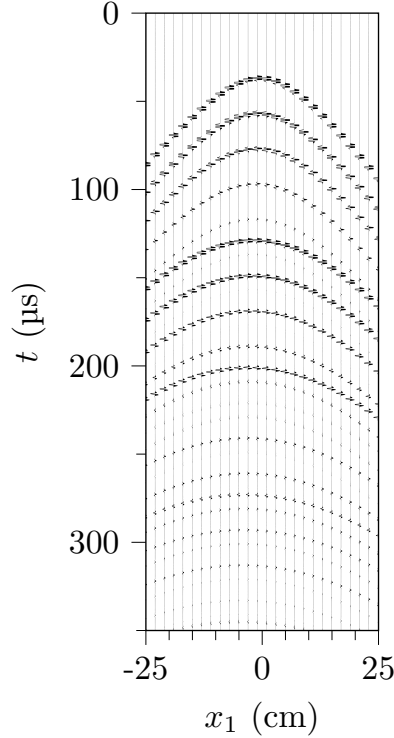


Figure 3. The modeled reflection response $R(\mathbf{x}, \mathbf{x}_S, t) * S(t)$ at $\partial\mathbb{D}_0$.

the function $\exp\{2t/350\mu s\}$. Note that the apices of the reflection hyperbolae drift to the left with increasing time, which is a manifestation of the non-reciprocal medium parameters. Because the medium is laterally invariant, the response to any other source at the surface is just a laterally shifted version of the response in Figure 3. We apply the Marchenko method, discussed in detail in the previous section, to derive the focusing functions $f_1^\pm(\mathbf{x}_S, \mathbf{x}_A, t)$ and $f_1^{\pm(a)}(\mathbf{x}_S, \mathbf{x}_A, t)$ for fixed $\mathbf{x}_S = (0, 0)$ and variable \mathbf{x}_A . As input we use the reflection response $R(\mathbf{x}, \mathbf{x}_S, t) * S(t)$ and the direct arrivals $T_d(\mathbf{x}_A, \mathbf{x}_S, t)$ and $T_d^{(a)}(\mathbf{x}_A, \mathbf{x}_S, t)$ modelled in the medium and its adjoint (in practice it suffices to model these in an estimated smooth background medium and its adjoint). For t_e in the time windows $w(\mathbf{x}_A, \mathbf{x}_S, t)$ and $w^{(a)}(\mathbf{x}_A, \mathbf{x}_S, t)$ we choose half the duration of the symmetric wavelet $S(t)$, i.e., $t_e = 0.65\mu s$, and the Heaviside functions are tapered. Because we consider a laterally invariant medium, the integrals in the right-hand sides of equations (32), (33), (37) and (38) are efficiently replaced by multiplications in the wavenumber-frequency domain. In total we apply 10 iterations of the Marchenko scheme to derive the focusing functions $f_1^\pm(\mathbf{x}_S, \mathbf{x}_A, t) * S(t)$ and the same number of iterations to derive $f_1^{\pm(a)}(\mathbf{x}_S, \mathbf{x}_A, t) * S(t)$. These focusing functions are substituted into equations (27) and (35) (of which the integrals are also evaluated via the wavenumber-frequency domain) to obtain the Green's functions $G^+(\mathbf{x}_A, \mathbf{x}_S, t) * S(t)$ and $G^-(\mathbf{x}_A, \mathbf{x}_S, t) * S(t)$. The superposition

of these Green's functions is shown in grey-level display in Figure 4 in the form of snapshots (i.e., wave fields at frozen time), for fixed $\mathbf{x}_S = (0, 0)$ and variable \mathbf{x}_A . The amplitudes are clipped at 20% of the maximum amplitude in each snapshot. This figure clearly shows the propagation of the wave field from the source through the layered non-reciprocal medium. The wavefronts are asymmetric as a result of the non-reciprocal medium parameters (for a reciprocal medium these snapshots would be symmetric with respect to the vertical dashed lines). Multiple scattering between the layer interfaces is also clearly visible. The interfaces, indicated by the solid horizontal lines in each of the panels in Figure 4, are only shown here to aid the interpretation of the retrieved Green's functions. However, no explicit information of these interfaces has been used to retrieve these Green's functions; all information about the scattering at the layer interfaces comes directly from the reflection response $R(\mathbf{x}, \mathbf{x}_S, t) * S(t)$. The amplitudes along the retrieved wave fronts deviate approximately 1 to 2% from a directly modelled Green's function, except directly below the interfaces (within half a wavelength), where errors can reach 50% (worst case) as a result of the window operations. The snapshots also exhibit some weak spurious linear events, which are mainly caused by the negligence of evanescent waves and the absence of very large propagation angles in the reflection response.

Next, we image the interfaces of the layered medium. First we use a primary imaging method, accounting for the non-reciprocal properties of the medium, applied directly to the reflection response of Figure 3. The result is shown in Figure 5(a). The three interfaces of the medium are imaged at the correct positions (indicated by the dotted lines), but there are also artefacts, indicated by the arrows. These artefacts are caused by the internal multiple reflections which are handled as primaries by standard imaging methods. Next, we use the retrieved downgoing and upgoing Green's functions $G^+(\mathbf{x}_A, \mathbf{x}_S, t) * S(t)$ and $G^-(\mathbf{x}_A, \mathbf{x}_S, t) * S(t)$ of Figure 4, derive $R(\mathbf{x}_A, \mathbf{x}, t)$ by inverting equation (41) (via the wavenumber-frequency domain) and select $R(\mathbf{x}, \mathbf{x}, t = 0)$ for $x_1 = 0$ and variable x_3 . The result is shown in Figure 5(b). Note that the artefacts related to the internal multiples have disappeared. For comparison, Figure 5(c) shows the true reflectivity, filtered with the same filters as used in both imaging methods. The Marchenko imaging result (Figure 5(b)) matches the true reflectivity significantly better than the result obtained with the primary imaging method (Figure 5(a)).

7 CONCLUSIONS

Marchenko imaging has recently been introduced as a novel approach to account for multiple scattering in multidimensional acoustic and electromagnetic imaging. Given the recent interest in non-reciprocal materials, here we have extended the Marchenko approach for non-reciprocal

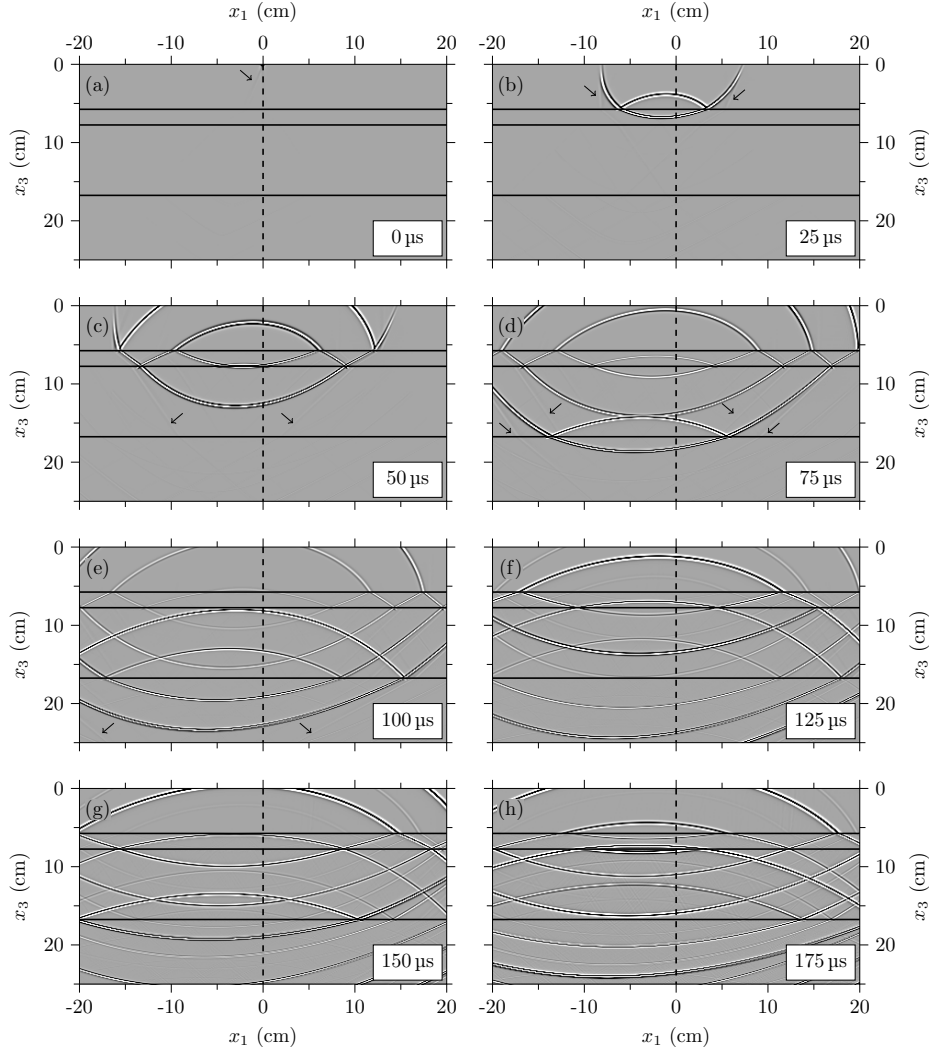


Figure 4. Snapshots of $\{G^+(\mathbf{x}_A, \mathbf{x}_S, t) + G^-(\mathbf{x}_A, \mathbf{x}_S, t)\} * S(t)$, retrieved via equations (27) and (35), for $\mathbf{x}_S = (0, 0)$ and variable \mathbf{x}_A .

media. We have derived two iterative Marchenko schemes, one to retrieve focusing functions in a truncated version of the actual medium and one to retrieve these functions in a truncated version of the adjoint medium. Both schemes use the reflection response of the actual medium as input, plus estimates of the direct arrivals of the transmission response of the truncated actual medium (for the first scheme) and of the truncated adjoint medium (for the second scheme). We have derived Green's function representations, which express the downgoing and upgoing part of the Green's function inside the non-reciprocal medium, in terms of the reflection response at the surface of the actual medium and the focusing functions in the truncated actual and adjoint medium. From these downgoing and upgoing Green's functions, a reflectivity image of the medium can be obtained. We have illustrated the proposed approach

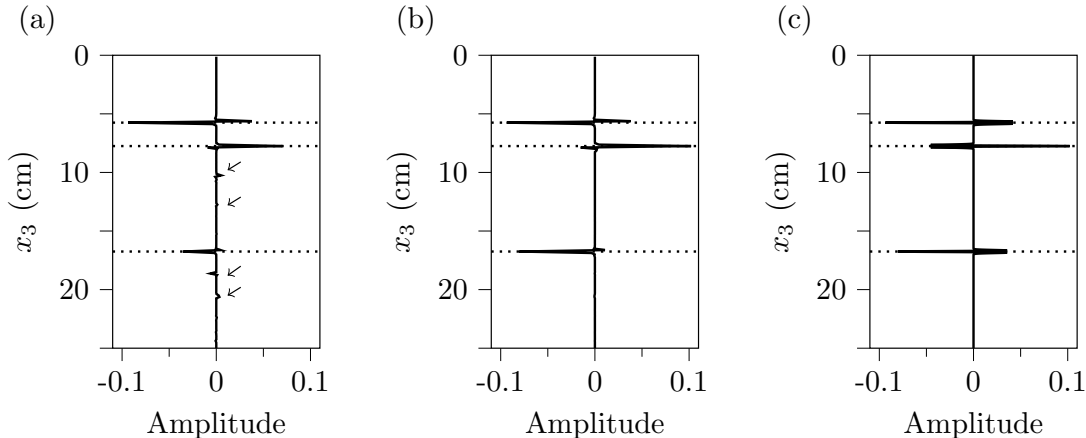


Figure 5. (a) Imaged reflectivity, using a primary imaging method. (b) Idem, Marchenko method. (c) True reflectivity.

at the hand of a numerical example for a horizontally layered non-reciprocal medium. This example shows an accurate Green’s function, propagating through the medium and scattering at its interfaces, retrieved from the reflection response at the surface. Moreover, it shows an accurately obtained artefact-free reflectivity image of the non-reciprocal medium, which confirms that the proposed method properly handles internal multiple scattering in a non-reciprocal medium.

ACKNOWLEDGEMENTS

We thank Evert Slob for his advise about electromagnetic waves in non-reciprocal media. This work has received funding from the European Union’s Horizon 2020 research and innovation programme: European Research Council (grant agreement 742703) and Marie Skłodowska-Curie (grant agreement 641943).

APPENDIX A: WAVE EQUATIONS FOR NON-RECIPROCAL MEDIA

We discuss wave equations for non-reciprocal media for (1) electromagnetic waves, (2) elastodynamic waves, and (3) acoustic waves. Next, we derive (4) a unified scalar wave equation for non-reciprocal media.

A1 Electromagnetic waves

We start with the Maxwell equations for electromagnetic waves,

$$\partial_t D_i - \epsilon_{ijk} \partial_j H_k = -J_i^e, \quad (\text{A.1})$$

$$\partial_t B_j + \epsilon_{jkl} \partial_k E_l = -J_j^m. \quad (\text{A.2})$$

Lower-case subscripts take the values 1, 2 and 3 and Einstein's summation convention applies to repeated subscripts. Exceptions are made for subscripts r , s and u , which only take the values 1 and 3, and for subscript t , which denotes time. In equations (A.1) and (A.2), $E_l = E_l(\mathbf{x}, t)$ is the electric field strength, $H_k = H_k(\mathbf{x}, t)$ the magnetic field strength, $D_i = D_i(\mathbf{x}, t)$ the electric flux density, $B_j = B_j(\mathbf{x}, t)$ the magnetic flux density, $J_i^e = J_i^e(\mathbf{x}, t)$ and $J_j^m = J_j^m(\mathbf{x}, t)$ are source functions in terms of external electric and magnetic current densities and, finally, ϵ_{ijk} is the alternating tensor (or Levi-Civita tensor), with $\epsilon_{123} = \epsilon_{312} = \epsilon_{231} = 1$, $\epsilon_{213} = \epsilon_{321} = \epsilon_{132} = -1$, and all other components being zero. For metamaterials, the field and source quantities in equations (A.1) and (A.2) are macroscopic quantities. These are sometimes denoted as $\langle H_k \rangle$ etc. (Willis 2011), but for notational convenience we drop the brackets. The effective constitutive relations for lossless metamaterials read (Kong 1972; Kiehn et al. 1991; Willis 2011)

$$D_i = \epsilon_{ij} E_j + \eta_{ij} B_j, \quad (\text{A.3})$$

$$H_k = \theta_{kl} E_l + \nu_{kl} B_l, \quad (\text{A.4})$$

where $\epsilon_{ij} = \epsilon_{ij}(\mathbf{x})$ is the permittivity, $\nu_{kl} = \nu_{kl}(\mathbf{x})$ the inverse permeability, and $\eta_{ij} = \eta_{ij}(\mathbf{x})$ and $\theta_{kl} = \theta_{kl}(\mathbf{x})$ are coupling parameters. The inverse permeability is related to the permeability $\mu_{jk} = \mu_{jk}(\mathbf{x})$ via

$$\mu_{jk} \nu_{kl} = \delta_{jl}, \quad (\text{A.5})$$

with δ_{jl} the Kronecker delta function. The medium parameters in equations (A.3) and (A.4) are effective parameters. In general they are anisotropic, even when they are isotropic at micro scale. For a non-reciprocal lossless metamaterial they are real-valued and obey the following symmetry relations (Birss & Shrubbsall 1967; Kong 1972; Slob & Wapenaar 2009)

$$\epsilon_{ij} = \epsilon_{ji}, \quad \nu_{kl} = \nu_{lk}, \quad \mu_{jk} = \mu_{kj}, \quad \eta_{ij} = -\theta_{ji}. \quad (\text{A.6})$$

We reorganise the constitutive relations into a set of explicit expressions for D_i and B_j . To this end we multiply both sides of equation (A.4) by μ_{jk} . Using equation (A.5) this gives

$$B_j = -\mu_{jk} \theta_{kl} E_l + \mu_{jk} H_k. \quad (\text{A.7})$$

Substitution into equation (A.3) gives

$$D_i = (\varepsilon_{il} - \eta_{ij}\mu_{jk}\theta_{kl})E_l + \eta_{ij}\mu_{jk}H_k. \quad (\text{A.8})$$

Equations (A.8) and (A.7) form a new set of effective constitutive relations (Lindell et al. 1995; Slob & Wapenaar 2012),

$$D_i = \varepsilon_{il}^o E_l + \xi_{ik} H_k, \quad (\text{A.9})$$

$$B_j = \zeta_{jl} E_l + \mu_{jk} H_k, \quad (\text{A.10})$$

with

$$\varepsilon_{il}^o = \varepsilon_{il} - \eta_{ij}\mu_{jk}\theta_{kl}, \quad (\text{A.11})$$

$$\xi_{ik} = \eta_{ij}\mu_{jk}, \quad (\text{A.12})$$

$$\zeta_{jl} = -\mu_{jk}\theta_{kl}. \quad (\text{A.13})$$

On account of equation (A.6), these parameters obey the following symmetry relations (Tellegen 1948; Kong 1972)

$$\varepsilon_{il}^o = \varepsilon_{li}^o, \quad \xi_{lj} = \zeta_{jl}. \quad (\text{A.14})$$

Substitution of constitutive relations (A.9) and (A.10) into Maxwell equations (A.1) and (A.2), using $\xi_{lj} = \zeta_{jl}$, gives

$$\varepsilon_{il}^o \partial_t E_l + \xi_{ik} \partial_t H_k - \epsilon_{ijk} \partial_j H_k = -J_i^e, \quad (\text{A.15})$$

$$\xi_{lj} \partial_t E_l + \mu_{jk} \partial_t H_k + \epsilon_{jkl} \partial_k E_l = -J_j^m. \quad (\text{A.16})$$

Next, we assume that the sources, medium parameters and wave fields are independent of the x_2 -coordinate. Furthermore, we assume $\varepsilon_{21}^o = \varepsilon_{23}^o = 0$, $\mu_{21} = \mu_{23} = 0$, $\xi_{11} = \xi_{22} = \xi_{33} = \xi_{13} = \xi_{31} = 0$. Then equation (A.15) for $i = 1, 2, 3$ (using $\varepsilon_{13}^o = \varepsilon_{31}^o$) and equation (A.16) for $j = 1, 2, 3$ (using $\mu_{13} = \mu_{31}$) yield six equations, describing wave propagation in the (x_1, x_3) -plane. These can be separated into two independent sets of equations, for transverse-electric (TE) waves (with wave field quantities E_2 , H_1 and H_3) and for transverse-magnetic (TM) waves (with wave field quantities H_2 , E_1 and E_3). For TE wave propagation in the (x_1, x_3) -plane we thus obtain

$$\varepsilon_{22}^o \partial_t E_2 + \xi_{21} \partial_t H_1 + \xi_{23} \partial_t H_3 + \partial_1 H_3 - \partial_3 H_1 = -J_2^e, \quad (\text{A.17})$$

$$\mu_{11} \partial_t H_1 + \mu_{31} \partial_t H_3 + \xi_{21} \partial_t E_2 - \partial_3 E_2 = -J_1^m, \quad (\text{A.18})$$

$$\mu_{31} \partial_t H_1 + \mu_{33} \partial_t H_3 + \xi_{23} \partial_t E_2 + \partial_1 E_2 = -J_3^m \quad (\text{A.19})$$

and for TM wave propagation in the (x_1, x_3) -plane

$$\mu_{22}\partial_t H_2 + \xi_{12}\partial_t E_1 + \xi_{32}\partial_t E_3 - \partial_1 E_3 + \partial_3 E_1 = -J_2^m, \quad (\text{A.20})$$

$$\varepsilon_{11}^o\partial_t E_1 + \varepsilon_{31}^o\partial_t E_3 + \xi_{12}\partial_t H_2 + \partial_3 H_2 = -J_1^e, \quad (\text{A.21})$$

$$\varepsilon_{31}^o\partial_t E_1 + \varepsilon_{33}^o\partial_t E_3 + \xi_{32}\partial_t H_2 - \partial_1 H_2 = -J_3^e. \quad (\text{A.22})$$

A2 Elastodynamic waves

We start with the equation of motion and the definition of strain rate

$$\partial_t p_i - \partial_j \tau_{ij} = F_i, \quad (\text{A.23})$$

$$\partial_t e_{kl} - \frac{1}{2}(\partial_k v_l + \partial_l v_k) = -h_{kl}. \quad (\text{A.24})$$

Here $p_i = p_i(\mathbf{x}, t)$ is the momentum density, $\tau_{ij} = \tau_{ij}(\mathbf{x}, t)$ the stress tensor, $e_{kl} = e_{kl}(\mathbf{x}, t)$ the strain tensor, $v_k = v_k(\mathbf{x}, t)$ the particle velocity and $F_i = F_i(\mathbf{x}, t)$ and $h_{kl} = h_{kl}(\mathbf{x}, t)$ are source functions in terms of external force and deformation-rate density. For metamaterials, the field and source quantities in equations (A.23) and (A.24) are macroscopic quantities. These are sometimes denoted as $\langle \tau_{ij} \rangle$ etc. (Willis 2012), but for notational convenience we drop the brackets. They obey the following symmetry relations

$$\tau_{ij} = \tau_{ji}, \quad e_{kl} = e_{lk}, \quad h_{kl} = h_{lk}. \quad (\text{A.25})$$

The effective constitutive relations for metamaterials read (Willis 2012; Norris et al. 2012; Nassar et al. 2017)

$$p_i = \rho_{ik} v_k + S_{ikl}^{(2)} e_{kl}, \quad (\text{A.26})$$

$$\tau_{mn} = S_{mnp}^{(1)} v_p + c_{mnpq} e_{pq}, \quad (\text{A.27})$$

where $\rho_{ik} = \rho_{ik}(\mathbf{x})$ is the mass density tensor, $c_{mnpq} = c_{mnpq}(\mathbf{x})$ the stiffness tensor and $S_{mnp}^{(1)} = S_{mnp}^{(1)}(\mathbf{x})$ and $S_{ikl}^{(2)} = S_{ikl}^{(2)}(\mathbf{x})$ are coupling parameters. The stiffness tensor is related to the compliance tensor $s_{klmn} = s_{klmn}(\mathbf{x})$ via

$$s_{klmn} c_{mnpq} = \frac{1}{2}(\delta_{kp} \delta_{lq} + \delta_{kq} \delta_{lp}). \quad (\text{A.28})$$

The medium parameters in equations (A.26) and (A.27) are effective parameters. In general they are anisotropic, even when they are isotropic at micro scale. An example of a non-reciprocal metamaterial is a phononic crystal of which the stiffness and mass density are modulated in a wave-like fashion (Nassar et al. 2017). For this situation, equations (A.26) and (A.27) are defined in a coordinate system that moves along with the modulating wave, so that the effective medium parameters in this coordinate system are time-independent. For a non-reciprocal lossless metamaterial the medium parameters are real-valued and obey the

following symmetry relations (Nassar et al. 2017)

$$\rho_{ik} = \rho_{ki}, \quad (\text{A.29})$$

$$c_{mnpq} = c_{nmpq} = c_{mnqp} = c_{pqmn}, \quad (\text{A.30})$$

$$s_{klmn} = s_{lkmn} = s_{klnm} = s_{mnkl}, \quad (\text{A.31})$$

$$S_{mnp}^{(1)} = S_{nmp}^{(1)}, \quad (\text{A.32})$$

$$S_{ikl}^{(2)} = S_{ilk}^{(2)}, \quad (\text{A.33})$$

$$S_{ikl}^{(2)} = -S_{kli}^{(1)}. \quad (\text{A.34})$$

We reorganise the constitutive relations into a set of explicit expressions for p_i and e_{kl} . To this end we multiply both sides of equation (A.27) by s_{klmn} . Using equations (A.28) and $e_{kl} = e_{lk}$ this gives

$$e_{kl} = -s_{klmn} S_{mnp}^{(1)} v_p + s_{klmn} \tau_{mn}. \quad (\text{A.35})$$

Substitution into equation (A.26) gives

$$p_i = (\rho_{ip} - S_{ikl}^{(2)} s_{klmn} S_{mnp}^{(1)}) v_p + S_{ikl}^{(2)} s_{klmn} \tau_{mn}. \quad (\text{A.36})$$

Equations (A.36) and (A.35) form a new set of effective constitutive relations,

$$p_i = \rho_{ip}^o v_p - \xi_{imn} \tau_{mn}, \quad (\text{A.37})$$

$$e_{kl} = -\zeta_{klp} v_p + s_{klmn} \tau_{mn}, \quad (\text{A.38})$$

with

$$\rho_{ip}^o = \rho_{ip} - S_{ikl}^{(2)} s_{klmn} S_{mnp}^{(1)}, \quad (\text{A.39})$$

$$\xi_{imn} = -S_{ikl}^{(2)} s_{klmn}, \quad (\text{A.40})$$

$$\zeta_{klp} = s_{klmn} S_{mnp}^{(1)}. \quad (\text{A.41})$$

For convenience we use the same symbols (ξ and ζ) for the coupling parameters as in the electromagnetic constitutive relations, but of course these are different quantities with different physical dimensions. On account of equations (A.29), (A.31) and (A.34) these parameters obey the following symmetry relations

$$\rho_{ip}^o = \rho_{pi}^o, \quad \zeta_{klp} = \zeta_{lkp}, \quad \xi_{imn} = \xi_{inm}, \quad \xi_{pkl} = \zeta_{klp}. \quad (\text{A.42})$$

Substitution of constitutive relations (A.37) and (A.38) into equations (A.23) and (A.24), using $\xi_{pkl} = \zeta_{klp}$, gives

$$\rho_{ip}^o \partial_t v_p - \xi_{imn} \partial_t \tau_{mn} - \partial_j \tau_{ij} = F_i, \quad (\text{A.43})$$

$$-\xi_{pkl} \partial_t v_p + s_{klmn} \partial_t \tau_{mn} - \frac{1}{2} (\partial_k v_l + \partial_l v_k) = -h_{kl}. \quad (\text{A.44})$$

Next, we assume that the sources, medium parameters and wave fields are independent of the x_2 -coordinate. Furthermore, we assume $\rho_{21}^o = \rho_{23}^o = 0$, $s_{1211} = s_{1222} = s_{1233} = s_{1213} = s_{3211} = s_{3222} = s_{3233} = s_{3213} = 0$ and $\xi_{112} = \xi_{132} = \xi_{211} = \xi_{222} = \xi_{233} = \xi_{213} = \xi_{312} = \xi_{332} = 0$. Then equation (A.43) for $i = 2$ (using $\xi_{2mn} = \xi_{2nm}$ and $\tau_{mn} = \tau_{nm}$) and equation (A.44) for $k = 1, 3$ (setting $l = 2$ in both cases and using equation (A.31)) yield three equations, describing the propagation of horizontally polarised shear (SH) waves (with wave field quantities v_2 , τ_{21} and τ_{23}) in the (x_1, x_3) -plane:

$$\rho_{22}^o \partial_t v_2 - 2\xi_{221} \partial_t \tau_{21} - 2\xi_{223} \partial_t \tau_{23} - \partial_1 \tau_{21} - \partial_3 \tau_{23} = F_2, \quad (\text{A.45})$$

$$-4s_{1221} \partial_t \tau_{21} - 4s_{1223} \partial_t \tau_{23} + 2\xi_{221} \partial_t v_2 + \partial_1 v_2 = 2h_{12}, \quad (\text{A.46})$$

$$-4s_{1223} \partial_t \tau_{21} - 4s_{3223} \partial_t \tau_{23} + 2\xi_{223} \partial_t v_2 + \partial_3 v_2 = 2h_{32}. \quad (\text{A.47})$$

A3 Acoustic waves

We derive the equations for acoustic waves from those for elastodynamic waves. To this end we make the following substitutions

$$\tau_{ij} = -\delta_{ij} \sigma, \quad (\text{A.48})$$

$$e_{kl} = \frac{1}{3} \delta_{kl} \Theta, \quad (\text{A.49})$$

$$h_{kl} = \frac{1}{3} \delta_{kl} q, \quad (\text{A.50})$$

$$c_{mnpq} = \delta_{mn} \delta_{pq} K. \quad (\text{A.51})$$

Here $\sigma = \sigma(\mathbf{x}, t)$ is the acoustic pressure, $\Theta = \Theta(\mathbf{x}, t)$ the cubic dilatation, $q = q(\mathbf{x}, t)$ a source function in terms of volume injection-rate density and $K = K(\mathbf{x})$ the effective bulk modulus of the medium. With these substitutions, equations (A.23) and (A.24) become

$$\partial_t p_i + \partial_i \sigma = F_i, \quad (\text{A.52})$$

$$\frac{1}{3} \delta_{kl} \partial_t \Theta - \frac{1}{2} (\partial_k v_l + \partial_l v_k) = -\frac{1}{3} \delta_{kl} q. \quad (\text{A.53})$$

Multiplying both sides of the latter equation by δ_{kl} we obtain

$$\partial_t \Theta - \partial_k v_k = -q. \quad (\text{A.54})$$

Similarly, the constitutive relations (A.26) and (A.27) become

$$p_i = \rho_{ik} v_k + \frac{1}{3} S_{ill}^{(2)} \Theta, \quad (\text{A.55})$$

$$-\delta_{mn} \sigma = S_{mnp}^{(1)} v_p + \frac{1}{3} \delta_{mn} \delta_{pq} K \delta_{pq} \Theta. \quad (\text{A.56})$$

Multiplying both sides of the latter equation by $\frac{1}{3} \delta_{mn}$ we obtain

$$-\sigma = \frac{1}{3} S_{mmp}^{(1)} v_p + K \Theta. \quad (\text{A.57})$$

On account of equations (A.29) and (A.34), the effective medium parameters in constitutive relations (A.55) and (A.57) obey the following symmetry relations

$$\rho_{ik} = \rho_{ki}, \quad S_{ill}^{(2)} = -S_{mmi}^{(1)}. \quad (\text{A.58})$$

We reorganise the constitutive relations into a set of explicit expressions for p_i and Θ . To this end we divide both sides of equation (A.57) by K , which gives

$$\Theta = -\zeta_p v_p - \kappa \sigma, \quad (\text{A.59})$$

with

$$\zeta_p = \frac{1}{3} \kappa S_{mmp}^{(1)}, \quad (\text{A.60})$$

$$\kappa = 1/K. \quad (\text{A.61})$$

Substitution into equation (A.55) gives

$$p_i = \rho_{ip}^o v_p + \xi_i \sigma, \quad (\text{A.62})$$

with

$$\rho_{ip}^o = \rho_{ip} - \frac{1}{9} \kappa S_{ill}^{(2)} S_{mmp}^{(1)}, \quad (\text{A.63})$$

$$\xi_i = -\frac{1}{3} \kappa S_{ill}^{(2)}. \quad (\text{A.64})$$

Equations (A.62) and (A.59) form a new set of constitutive relations. On account of equation (A.58), the medium parameters in these relations obey the following symmetry relations

$$\rho_{ip}^o = \rho_{pi}^o, \quad \xi_p = \zeta_p. \quad (\text{A.65})$$

Substitution of constitutive relations (A.62) and (A.59) into equations (A.52) and (A.54), using $\xi_p = \zeta_p$, gives

$$\rho_{ip}^o \partial_t v_p + \xi_i \partial_t \sigma + \partial_i \sigma = F_i, \quad (\text{A.66})$$

$$\xi_p \partial_t v_p + \kappa \partial_t \sigma + \partial_k v_k = q. \quad (\text{A.67})$$

Next, we assume that the sources, medium parameters and wave fields are independent of the x_2 -coordinate. Furthermore, we assume $\rho_{12}^o = \rho_{32}^o = 0$ and $\xi_2 = 0$. Then equation (A.66) for $i = 1, 3$ (using $\rho_{13}^o = \rho_{31}^o$) and equation (A.67) yield three equations, describing the propagation of acoustic (AC) waves (with wave field quantities σ , v_1 and v_3) in the (x_1, x_3) -plane:

$$\kappa \partial_t \sigma + \xi_1 \partial_t v_1 + \xi_3 \partial_t v_3 + \partial_1 v_1 + \partial_3 v_3 = q, \quad (\text{A.68})$$

$$\rho_{11}^o \partial_t v_1 + \rho_{31}^o \partial_t v_3 + \xi_1 \partial_t \sigma + \partial_1 \sigma = F_1, \quad (\text{A.69})$$

$$\rho_{31}^o \partial_t v_1 + \rho_{33}^o \partial_t v_3 + \xi_3 \partial_t \sigma + \partial_3 \sigma = F_3. \quad (\text{A.70})$$

A4 Unified scalar wave equation

The systems of equations for transverse-electric waves (TE waves, equations (A.17) – (A.19)), transverse-magnetic waves (TM waves, equations (A.20) – (A.22)), horizontally polarised shear waves (SH waves, equations (A.45) – (A.47)) and acoustic waves (AC waves, equations (A.68) – (A.70)), can all be cast in the following form

$$\alpha \partial_t P + (\partial_r + \gamma_r \partial_t) Q_r = B, \quad (\text{A.71})$$

$$(\partial_s + \gamma_s \partial_t) P + \beta_{su} \partial_t Q_u = C_s, \quad (\text{A.72})$$

with $\beta_{su} = \beta_{us}$. Recall that subscripts r , s and u only take the values 1 and 3. The field quantities, medium parameters and source functions in these equations are given in Table 1 for TE, TM, SH and AC waves. We derive a scalar wave equation for P by eliminating Q_r from equations (A.71) and (A.72). We define the inverse of β_{su} via

$$\vartheta_{rs} \beta_{su} = \delta_{ru}. \quad (\text{A.73})$$

Because β_{su} is a symmetric 2×2 tensor, the following simple expressions hold for ϑ_{rs}

$$\vartheta_{11} = \beta_{33} / \Delta, \quad (\text{A.74})$$

$$\vartheta_{13} = \vartheta_{31} = -\beta_{31} / \Delta, \quad (\text{A.75})$$

$$\vartheta_{33} = \beta_{11} / \Delta, \quad (\text{A.76})$$

with

$$\Delta = \beta_{11} \beta_{33} - \beta_{31}^2. \quad (\text{A.77})$$

Apply ∂_t to both sides of equation (A.71) and $(\partial_r + \gamma_r \partial_t) \vartheta_{rs}$ to both sides of equation (A.72) and subtract the results. Using the fact that the effective medium parameters are time-independent, this gives

$$(\partial_r + \gamma_r \partial_t) \vartheta_{rs} (\partial_s + \gamma_s \partial_t) P - \alpha \partial_t^2 P = (\partial_r + \gamma_r \partial_t) \vartheta_{rs} C_s - \partial_t B. \quad (\text{A.78})$$

APPENDIX B: DECOMPOSITION OF THE RECIPROCITY THEOREMS FOR NON-RECIPROCAL MEDIA

We (1) derive a unified matrix-vector wave equation for non-reciprocal media, (2) apply decomposition to the operator matrix, and (3) use the symmetry properties of the decomposed operators to derive reciprocity theorems for decomposed wave fields.

B1 Unified matrix-vector wave equation

Using the Fourier transform, defined in equation (5), we transform equations (A.71) and (A.72) to the space-frequency domain, yielding

$$-i\omega\alpha P + (\partial_r - i\omega\gamma_r)Q_r = B, \quad (\text{B.1})$$

$$(\partial_s - i\omega\gamma_s)P - i\omega\beta_{su}Q_u = C_s. \quad (\text{B.2})$$

We derive a matrix-vector wave equation of the form

$$\partial_3 \mathbf{q} = \mathcal{A} \mathbf{q} + \mathbf{d}, \quad (\text{B.3})$$

with wave vector $\mathbf{q} = \mathbf{q}(\mathbf{x}, \omega)$ and source vector $\mathbf{d} = \mathbf{d}(\mathbf{x}, \omega)$ defined as

$$\mathbf{q} = \begin{pmatrix} P \\ Q_3 \end{pmatrix}, \quad \mathbf{d} = \begin{pmatrix} C^o \\ B^o \end{pmatrix} \quad (\text{B.4})$$

and operator matrix $\mathcal{A} = \mathcal{A}(\mathbf{x}, \omega)$ defined as

$$\mathcal{A} = \begin{pmatrix} \mathcal{A}_{11} & \mathcal{A}_{12} \\ \mathcal{A}_{21} & \mathcal{A}_{22} \end{pmatrix}. \quad (\text{B.5})$$

We separate the derivatives in the x_3 -direction from the derivatives in the x_1 -direction in equations (B.1) and (B.2), the latter multiplied by $\vartheta_{33}^{-1}\vartheta_{3s}$ on both sides. Hence,

$$\partial_3 Q_3 = i\omega\alpha P + i\omega\gamma_r Q_r - \partial_1 Q_1 + B, \quad (\text{B.6})$$

$$\partial_3 P = -\vartheta_{33}^{-1}(-i\omega Q_3 - i\omega\vartheta_{3s}\gamma_s P + \vartheta_{31}\partial_1 P - \vartheta_{3s}C_s). \quad (\text{B.7})$$

Q_1 needs to be eliminated from equation (B.6). From equation (B.2), multiplied on both sides by ϑ_{1s} , we obtain

$$Q_1 = \frac{1}{i\omega}(-i\omega\vartheta_{1s}\gamma_s P + \vartheta_{1s}\partial_s P - \vartheta_{1s}C_s). \quad (\text{B.8})$$

Substitution of equation (B.8) into (B.6) gives

$$\partial_3 Q_3 = i\omega\alpha P + i\omega\gamma_3 Q_3 - \frac{1}{i\omega}(\partial_1 - i\omega\gamma_1)(-i\omega\vartheta_{1s}\gamma_s P + \vartheta_{1s}\partial_s P - \vartheta_{1s}C_s) + B, \quad (\text{B.9})$$

or, upon substitution of equation (B.7) and some reorganization,

$$\begin{aligned} \partial_3 Q_3 &= \left(i\omega\alpha - \frac{1}{i\omega}(\partial_1 - i\omega\gamma_1)b_1(\partial_1 - i\omega\gamma_1) \right) P \\ &\quad + \left(i\omega\gamma_3 - (\partial_1 - i\omega\gamma_1)\vartheta_{13}\vartheta_{33}^{-1} \right) Q_3 + B + \frac{1}{i\omega}(\partial_1 - i\omega\gamma_1)b_s C_s, \end{aligned} \quad (\text{B.10})$$

with

$$b_s = \vartheta_{1s} - \vartheta_{13}\vartheta_{33}^{-1}\vartheta_{3s}, \quad (\text{B.11})$$

or, using equations (A.74) – (A.77),

$$b_1 = 1/\beta_{11}, \quad (\text{B.12})$$

$$b_3 = 0. \quad (\text{B.13})$$

Equations (B.7) and (B.10) can be cast in the form of the matrix-vector wave equation defined in equations (B.3) – (B.5), with

$$\mathcal{A}_{11} = i\omega\gamma_3 - d(\partial_1 - i\omega\gamma_1), \quad (\text{B.14})$$

$$\mathcal{A}_{12} = i\omega\vartheta_{33}^{-1}, \quad (\text{B.15})$$

$$\mathcal{A}_{21} = i\omega\alpha - \frac{1}{i\omega}(\partial_1 - i\omega\gamma_1)b_1(\partial_1 - i\omega\gamma_1), \quad (\text{B.16})$$

$$\mathcal{A}_{22} = i\omega\gamma_3 - (\partial_1 - i\omega\gamma_1)d, \quad (\text{B.17})$$

$$C^o = dC_1 + C_3, \quad (\text{B.18})$$

$$B^o = B + \frac{1}{i\omega}(\partial_1 - i\omega\gamma_1)b_1C_1, \quad (\text{B.19})$$

with

$$d = \vartheta_{33}^{-1}\vartheta_{13} = -\beta_{31}/\beta_{11}. \quad (\text{B.20})$$

The notation in the right-hand side of equations (B.14) – (B.17) should be understood in the sense that differential operators act on all factors to the right of it. For example, the operator $\partial_1 b_1 \partial_1$ in equation (B.16), applied via equation (B.3) to the wave field P , implies $\partial_1(b_1 \partial_1 P)$.

B2 Decomposition of the operator matrix

We define the spatial Fourier transform of a function $f(\mathbf{x}, \omega)$ as

$$\tilde{f}(s_1, x_3, \omega) = \int_{-\infty}^{\infty} \exp(-i\omega s_1 x_1) f(\mathbf{x}, \omega) dx_1, \quad (\text{B.21})$$

with s_1 being the horizontal slowness. We use equation (B.21) to transform the operator matrix \mathcal{A} defined in equation (B.5) to the slowness domain, assuming the medium is laterally invariant at depth level x_3 . The spatial differential operators ∂_1 are thus replaced by $i\omega s_1$, hence

$$\tilde{\mathcal{A}}(s_1, x_3, \omega) = \begin{pmatrix} i\omega\{\gamma_3 - d(s_1 - \gamma_1)\} & i\omega\vartheta_{33}^{-1} \\ i\omega\vartheta_{33}s_3^2 & i\omega\{\gamma_3 - d(s_1 - \gamma_1)\} \end{pmatrix}, \quad (\text{B.22})$$

with

$$s_3^2 = \vartheta_{33}^{-1}(\alpha - b_1(s_1 - \gamma_1)^2). \quad (\text{B.23})$$

The eigenvalue decomposition of $\tilde{\mathcal{A}}$ reads

$$\tilde{\mathcal{A}} = \tilde{\mathcal{L}}\tilde{\mathcal{H}}\tilde{\mathcal{L}}^{-1}. \quad (\text{B.24})$$

Using the standard approach to find eigenvalues and eigenvectors we obtain

$$\tilde{\mathcal{H}}(s_1, x_3, \omega) = \begin{pmatrix} i\omega\lambda^+ & 0 \\ 0 & -i\omega\lambda^- \end{pmatrix}, \quad (\text{B.25})$$

$$\tilde{\mathcal{L}}(s_1, x_3, \omega) = \frac{1}{\sqrt{2}} \begin{pmatrix} 1/\sqrt{\vartheta_{33}s_3} & 1/\sqrt{\vartheta_{33}s_3} \\ \sqrt{\vartheta_{33}s_3} & -\sqrt{\vartheta_{33}s_3} \end{pmatrix}, \quad (\text{B.26})$$

$$\{\tilde{\mathcal{L}}(s_1, x_3, \omega)\}^{-1} = \frac{1}{\sqrt{2}} \begin{pmatrix} \sqrt{\vartheta_{33}s_3} & 1/\sqrt{\vartheta_{33}s_3} \\ \sqrt{\vartheta_{33}s_3} & -1/\sqrt{\vartheta_{33}s_3} \end{pmatrix}, \quad (\text{B.27})$$

where

$$\lambda^\pm = s_3 \pm \{\gamma_3 - d(s_1 - \gamma_1)\}, \quad (\text{B.28})$$

$$s_3 = \begin{cases} +\sqrt{\vartheta_{33}^{-1}(\alpha - b_1(s_1 - \gamma_1)^2)}, & \text{for } (s_1 - \gamma_1)^2 \leq \frac{\alpha}{b_1}, \\ +i\sqrt{\vartheta_{33}^{-1}(b_1(s_1 - \gamma_1)^2 - \alpha)}, & \text{for } (s_1 - \gamma_1)^2 > \frac{\alpha}{b_1}. \end{cases} \quad (\text{B.29})$$

Note that the intervals $(s_1 - \gamma_1)^2 \leq \frac{\alpha}{b_1}$ and $(s_1 - \gamma_1)^2 > \frac{\alpha}{b_1}$ in equation (B.29) represent propagating and evanescent waves, respectively.

B3 Reciprocity theorems for decomposed wave fields

We derive reciprocity theorems for downgoing and upgoing wave fields, exploiting the symmetry properties of operator $\tilde{\mathcal{L}}$. Reciprocity theorems (15) and (16) can be compactly written as

$$\int_{\partial\mathbb{D}_0} \{\mathbf{q}_A^{(a)}\}^t \mathbf{N} \mathbf{q}_B dx_1 = \int_{\partial\mathbb{D}_A} \{\mathbf{q}_A^{(a)}\}^t \mathbf{N} \mathbf{q}_B dx_1 \quad (\text{B.30})$$

and

$$\int_{\partial\mathbb{D}_0} \mathbf{q}_A^\dagger \mathbf{K} \mathbf{q}_B dx_1 = \int_{\partial\mathbb{D}_A} \mathbf{q}_A^\dagger \mathbf{K} \mathbf{q}_B dx_1, \quad (\text{B.31})$$

with \mathbf{q} defined in equation (18), superscript t denoting transposition, \dagger transposition and complex conjugation, and matrices \mathbf{N} and \mathbf{K} defined as

$$\mathbf{N} = \begin{pmatrix} 0 & 1 \\ -1 & 0 \end{pmatrix}, \quad \mathbf{K} = \begin{pmatrix} 0 & 1 \\ 1 & 0 \end{pmatrix}. \quad (\text{B.32})$$

According to equation (17), vector \mathbf{q} is (for both states) related to vector \mathbf{p} via $\mathbf{q} = \mathcal{L}\mathbf{p}$, with \mathbf{p} defined in equation (18). Here we use this relation and the symmetry properties of composition operator $\tilde{\mathcal{L}}$ to recast equations (B.30) and (B.31) into reciprocity theorems for downgoing and upgoing wave fields.

Using the spatial Fourier transform, defined in equation (B.21), and Parseval's theorem,

we first rewrite the integrals in equations (B.30) and (B.31) as

$$\int_{-\infty}^{\infty} \{\mathbf{q}_A^{(a)}(x_1, x_3, \omega)\}^t \mathbf{N} \mathbf{q}_B(x_1, x_3, \omega) dx_1 = \tag{B.33}$$

$$\frac{\omega}{2\pi} \int_{-\infty}^{\infty} \{\tilde{\mathbf{q}}_A^{(a)}(-s_1, x_3, \omega)\}^t \mathbf{N} \tilde{\mathbf{q}}_B(s_1, x_3, \omega) ds_1$$

and

$$\int_{-\infty}^{\infty} \{\mathbf{q}_A(x_1, x_3, \omega)\}^\dagger \mathbf{K} \mathbf{q}_B(x_1, x_3, \omega) dx_1 = \tag{B.34}$$

$$\frac{\omega}{2\pi} \int_{-\infty}^{\infty} \{\tilde{\mathbf{q}}_A(s_1, x_3, \omega)\}^\dagger \mathbf{K} \tilde{\mathbf{q}}_B(s_1, x_3, \omega) ds_1,$$

respectively, where x_3 can represent the depth level of $\partial\mathbb{D}_0$ or $\partial\mathbb{D}_A$. Assuming the medium parameters are laterally invariant at x_3 , the composition operation $\mathbf{q} = \mathbf{L}\mathbf{p}$ can be rewritten in the slowness domain as

$$\tilde{\mathbf{q}}(s_1, x_3, \omega) = \tilde{\mathcal{L}}(s_1, x_3, \omega) \tilde{\mathbf{p}}(s_1, x_3, \omega), \tag{B.35}$$

with $\tilde{\mathcal{L}}(s_1, x_3, \omega)$ defined in equation (B.26). Substituting this in the right-hand sides of equations (B.33) and (B.34) yields

$$\frac{\omega}{2\pi} \int_{-\infty}^{\infty} \{\tilde{\mathbf{q}}_A^{(a)}(-s_1, x_3, \omega)\}^t \mathbf{N} \tilde{\mathbf{q}}_B(s_1, x_3, \omega) ds_1 = \tag{B.36}$$

$$\frac{\omega}{2\pi} \int_{-\infty}^{\infty} \{\tilde{\mathbf{p}}_A^{(a)}(-s_1, x_3, \omega)\}^t \{\tilde{\mathcal{L}}^{(a)}(-s_1, x_3, \omega)\}^t \mathbf{N} \tilde{\mathcal{L}}(s_1, x_3, \omega) \tilde{\mathbf{p}}_B(s_1, x_3, \omega) ds_1$$

and

$$\frac{\omega}{2\pi} \int_{-\infty}^{\infty} \{\tilde{\mathbf{q}}_A(s_1, x_3, \omega)\}^\dagger \mathbf{K} \tilde{\mathbf{q}}_B(s_1, x_3, \omega) ds_1 = \tag{B.37}$$

$$\frac{\omega}{2\pi} \int_{-\infty}^{\infty} \{\tilde{\mathbf{p}}_A(s_1, x_3, \omega)\}^\dagger \{\tilde{\mathcal{L}}(s_1, x_3, \omega)\}^\dagger \mathbf{K} \tilde{\mathcal{L}}(s_1, x_3, \omega) \tilde{\mathbf{p}}_B(s_1, x_3, \omega) ds_1,$$

respectively. From the definition of $\tilde{\mathcal{L}}(s_1, x_3, \omega)$ in equation (B.26), with s_3 defined in equation (B.29), recalling that superscript (a) implies that γ_r is replaced by $-\gamma_r$, we find

$$\{\tilde{\mathcal{L}}^{(a)}(-s_1, x_3, \omega)\}^t \mathbf{N} \tilde{\mathcal{L}}(s_1, x_3, \omega) = -\mathbf{N}, \quad \text{for } -\infty < s_1 < \infty, \tag{B.38}$$

$$\{\tilde{\mathcal{L}}(s_1, x_3, \omega)\}^\dagger \mathbf{K} \tilde{\mathcal{L}}(s_1, x_3, \omega) = \mathbf{J}, \quad \text{for } (s_1 - \gamma_1)^2 \leq \frac{\alpha}{b_1}, \tag{B.39}$$

with \mathbf{J} defined as

$$\mathbf{J} = \begin{pmatrix} 1 & 0 \\ 0 & -1 \end{pmatrix}. \tag{B.40}$$

Note that equation (B.38) holds for propagating and evanescent waves, whereas equation (B.39) holds for propagating waves only. Substituting equations (B.38) and (B.39) into equa-

tions (B.36) and (B.37) and using Parseval's theorem again yields

$$\begin{aligned} \int_{-\infty}^{\infty} \{\mathbf{q}_A^{(a)}(x_1, x_3, \omega)\}^t \mathbf{N} \mathbf{q}_B(x_1, x_3, \omega) dx_1 = \\ - \int_{-\infty}^{\infty} \{\mathbf{p}_A^{(a)}(x_1, x_3, \omega)\}^t \mathbf{N} \mathbf{p}_B(x_1, x_3, \omega) dx_1 \end{aligned} \quad (\text{B.41})$$

and

$$\begin{aligned} \int_{-\infty}^{\infty} \{\mathbf{q}_A(x_1, x_3, \omega)\}^\dagger \mathbf{K} \mathbf{q}_B(x_1, x_3, \omega) dx_1 = \\ \int_{-\infty}^{\infty} \{\mathbf{p}_A(x_1, x_3, \omega)\}^\dagger \mathbf{J} \mathbf{p}_B(x_1, x_3, \omega) dx_1, \end{aligned} \quad (\text{B.42})$$

respectively. Equation (B.41) is exact, whereas in equation (B.42) evanescent waves are neglected. Using these equations at boundaries $\partial\mathbb{D}_0$ and $\partial\mathbb{D}_A$ in reciprocity theorems (B.30) and (B.31) yields

$$\int_{\partial\mathbb{D}_0} \{\mathbf{p}_A^{(a)}\}^t \mathbf{N} \mathbf{p}_B dx_1 = \int_{\partial\mathbb{D}_A} \{\mathbf{p}_A^{(a)}\}^t \mathbf{N} \mathbf{p}_B dx_1 \quad (\text{B.43})$$

and

$$\int_{\partial\mathbb{D}_0} \mathbf{p}_A^\dagger \mathbf{J} \mathbf{p}_B dx_1 = \int_{\partial\mathbb{D}_A} \mathbf{p}_A^\dagger \mathbf{J} \mathbf{p}_B dx_1, \quad (\text{B.44})$$

respectively. Substituting the expressions for \mathbf{p} (equation 18), \mathbf{N} (equation B.32) and \mathbf{J} (equation B.40) we obtain the reciprocity theorems of equations (19) and (20) for the downgoing and upgoing fields U^+ and U^- .

REFERENCES

- Achenbach, J. D., 2003. *Reciprocity in elastodynamics*, Cambridge University Press.
- Amundsen, L., 2001. Elimination of free-surface related multiples without need of the source wavelet, *Geophysics*, **66**(1), 327–341.
- Ardakani, A. G., 2014. Nonreciprocal electromagnetic wave propagation in one-dimensional ternary magnetized plasma photonic crystals, *Journal of the Optical Society of America B*, **31**, 332–339.
- Attarzadeh, M. A. & Nouh, M., 2018. Non-reciprocal elastic wave propagation in 2D phononic membranes with spatiotemporally varying material properties, *Journal of Sound and Vibration*, **2018**, 264–277.
- Behura, J., Wapenaar, K., & Snieder, R., 2014. Autofocus imaging: Image reconstruction based on inverse scattering theory, *Geophysics*, **79**(3), A19–A26.
- Berkhout, A. J., 2014. Review paper: An outlook on the future of seismic imaging, Part II: Full-Wavefield Migration, *Geophysical Prospecting*, **62**, 931–949.
- Berkhout, A. J. & van Wulfften Palthe, D. W., 1979. Migration in terms of spatial deconvolution, *Geophysical Prospecting*, **27**(1), 261–291.

- Biersteker, J., 2001. MAGIC: Shell's surface multiple attenuation technique, in *SEG, Expanded Abstracts*, pp. 1301–1304.
- Birss, R. R. & Shrubbsall, R. G., 1967. The propagation of EM waves in magnetoelectric crystals, *Phil. Mag.*, **15**, 687–700.
- Bleistein, N. & Cohen, J. K., 1982. Velocity inversion - Present status, new directions, *Geophysics*, **47**, 1497–1511.
- Broggini, F. & Snieder, R., 2012. Connection of scattering principles: a visual and mathematical tour, *European Journal of Physics*, **33**, 593–613.
- Broggini, F., Snieder, R., & Wapenaar, K., 2014. Data-driven wavefield focusing and imaging with multidimensional deconvolution: Numerical examples for reflection data with internal multiples, *Geophysics*, **79**(3), WA107–WA115.
- Carvalho, P. M., Weglein, A. B., & Stolt, R. H., 1992. Nonlinear inverse scattering for multiple suppression: Application to real data, Part 1, in *SEG, Expanded Abstracts*, pp. 1093–1095.
- Claerbout, J. F., 1971. Toward a unified theory of reflector mapping, *Geophysics*, **36**, 467–481.
- Corones, J. P., Davison, M. E., & Krueger, R. J., 1983. Direct and inverse scattering in the time domain via invariant imbedding equations, *Journal of the Acoustical Society of America*, **74**, 1535–1541.
- Davydenko, M. & Verschuur, D. J., 2017. Full-wavefield migration: using surface and internal multiples in imaging, *Geophysical Prospecting*, **65**, 7–21.
- de Hoop, A. T., 1995. *Handbook of radiation and scattering of waves*, Academic Press, London.
- de Hoop, M. V., 1992. *Directional Decomposition of Transient Acoustic Wave Fields*, Ph.D. thesis, Delft University of Technology.
- de Hoop, M. V., 1996. Generalization of the Bremmer coupling series, *J. Math. Phys.*, **37**, 3246–3282.
- Devaney, A. J., 1982. A filtered backpropagation algorithm for diffraction tomography, *Ultrasonic Imaging*, **4**, 336–350.
- Dragoset, B., Verschuur, E., Moore, I., & Bisley, R., 2010. A perspective on 3D surface-related multiple elimination, *Geophysics*, **75**, 75A245–75A261.
- Elison, P., van Manen, D. J., Robertsson, J. O. A., Dukalski, M. S., & de Vos, K., 2018. Marchenko-based immersive wave simulation, *Geophysical Journal International*, **215**, 1118–1131.
- Esmersoy, C. & Oristaglio, M., 1988. Reverse-time wave-field extrapolation, imaging, and inversion, *Geophysics*, **53**, 920–931.
- Etgen, J., Gray, S. H., & Zhang, Y., 2009. An overview of depth imaging in exploration geophysics, *Geophysics*, **74**(6), WCA5–WCA17.
- Fishman, L., 1993. One-way propagation methods in direct and inverse scalar wave propagation modeling, *Radio Science*, **28**(5), 865–876.
- Fishman, L., McCoy, J. J., & Wales, S. C., 1987. Factorization and path integration of the Helmholtz equation: Numerical algorithms, *Journal of the Acoustical Society of America*, **81**(5), 1355–1376.

- Fishman, L., de Hoop, M. V., & van Stralen, M. J. N., 2000. Exact constructions of square-root Helmholtz operator symbols: The focusing quadratic profile, *J. Math. Phys.*, **41**(7), 4881–4938.
- Fokkema, J. T. & van den Berg, P. M., 1993. *Seismic applications of acoustic reciprocity*, Elsevier, Amsterdam.
- Godin, O. A., 1997. Reciprocity and energy theorems for waves in a compressible inhomogeneous moving fluid, *Wave Motion*, **25**, 143–167.
- Haines, A. J. & de Hoop, M. V., 1996. An invariant imbedding analysis of general wave scattering problems, *J. Math. Phys.*, **37**, 3854–3881.
- He, C., Lu, M. H., Heng, X., Feng, L., & Chen, Y. F., 2011. Parity-time electromagnetic diodes in a two-dimensional nonreciprocal photonic crystal, *Phys. Rev. B*, **83**, 075117.
- Holvik, E. & Amundsen, L., 2005. Elimination of the overburden response from multicomponent source and receiver seismic data, with source signature and decomposition into PP-, PS-, SP-, and SS-wave responses, *Geophysics*, **70**(2), S43–S59.
- Kennett, B. L. N. & Kerry, N. J., 1979. Seismic waves in a stratified half-space, *Geophysical Journal of the Royal Astronomical Society*, **57**, 557–584.
- Kiehn, R. M., Kiehn, G. P., & Roberds, J. B., 1991. Parity and time-reversal symmetry breaking, singular solutions, and Fresnel surfaces, *Physical Review A*, **43**(10), 5665–5671.
- Kong, J. A., 1972. Theorems of bianisotropic media, *Proc. IEEE*, **60**(9), 1036–1046.
- Langenberg, K. J., Berger, M., Kreutter, T., Mayer, K., & Schmitz, V., 1986. Synthetic aperture focusing technique signal processing, *NDT International*, **19**(3), 177–189.
- Lindell, I. V., Sihvola, A. H., & Suchy, K., 1995. Six-vector formalism in electromagnetics of bi-anisotropic media, *Journal of Electromagnetic Waves and Applications*, **9**(7-8), 887–903.
- Lindsey, C. & Braun, D. C., 2004. Principles of seismic holography for diagnostics of the shallow subphotosphere, *The Astrophysical Journal Supplement Series*, **155**(1), 209–225.
- Lyamshev, L. M., 1961. On some integral relationships in acoustics of moving medium, *Doklady Akademii Nauk*, **138**, 575–578.
- Maynard, J. D., Williams, E. G., & Lee, Y., 1985. Nearfield acoustic holography: I. Theory of generalized holography and the development of NAH, *Journal of the Acoustical Society of America*, **78**(4), 1395–1413.
- McMechan, G. A., 1983. Migration by extrapolation of time-dependent boundary values, *Geophysical Prospecting*, **31**, 413–420.
- Meles, G. A., Löer, K., Ravasi, M., Curtis, A., & da Costa Filho, C. A., 2015. Internal multiple prediction and removal using Marchenko autofocusing and seismic interferometry, *Geophysics*, **80**(1), A7–A11.
- Mildner, C., Brogini, F., Robertsson, J. O. A., van Manen, D. J., & Greenhalgh, S., 2017. Target-oriented velocity analysis using Marchenko-redatumed data, *Geophysics*, **82**(2), R75–R86.
- Nassar, H., Xu, X. C., Norris, A. N., & Huang, G. L., 2017. Modulated phononic crystals: Non-

- reciprocal wave propagation and Willis materials, *Journal of the Mechanics and Physics of Solids*, **101**, 10–29.
- Norris, A. N., Shuvalov, A. L., & Kutsenko, A. A., 2012. Analytical formulation of three-dimensional dynamic homogenization for periodic elastic systems, *Proceedings of the Royal Society A*, **468**, 1629–1651.
- Norton, S. J., 1992. Annular array imaging with full-aperture resolution, *Journal of the Acoustical Society of America*, **92**, 3202–3206.
- Oristaglio, M. L., 1989. An inverse scattering formula that uses all the data, *Inverse Problems*, **5**, 1097–1105.
- Pica, A., Poulain, G., David, B., Magesan, M., Baldock, S., Weisser, T., Hugonnet, P., & Herrmann, P., 2005. 3D surface-related multiple modeling, *The Leading Edge*, **24**(3), 292–296.
- Ravasi, M., 2017. Rayleigh-Marchenko redatuming for target-oriented, true-amplitude imaging, *Geophysics*, **82**(6), S439–S452.
- Ravasi, M., Meles, G., Curtis, A., Rawlinson, Z., & Yikuo, L., 2015. Seismic interferometry by multidimensional deconvolution without wavefield separation, *Geophysical Journal International*, **202**, 1–16.
- Ravasi, M., Vasconcelos, I., Kritski, A., Curtis, A., da Costa Filho, C. A., & Meles, G. A., 2016. Target-oriented Marchenko imaging of a North Sea field, *Geophysical Journal International*, **205**, 99–104.
- Rose, J. H., 2001. “Single-sided” focusing of the time-dependent Schrödinger equation, *Physical Review A*, **65**, 012707.
- Rose, J. H., 2002. ‘Single-sided’ autofocusing of sound in layered materials, *Inverse Problems*, **18**, 1923–1934.
- Singh, S., Snieder, R., van der Neut, J., Thorbecke, J., Slob, E., & Wapenaar, K., 2017. Accounting for free-surface multiples in Marchenko imaging, *Geophysics*, **82**(1), R19–R30.
- Slob, E. & Wapenaar, K., 2009. Retrieving the Green’s function from cross correlation in a bianisotropic medium, *Progress In Electromagnetics Research, PIER*, **93**, 255–274.
- Slob, E. & Wapenaar, K., 2012. Green’s function extraction for interfaces with impedance boundary conditions, *IEEE Trans. Ant. Prop.*, **60**(1), 351–359.
- Slob, E., Wapenaar, K., Broggini, F., & Snieder, R., 2014. Seismic reflector imaging using internal multiples with Marchenko-type equations, *Geophysics*, **79**(2), S63–S76.
- Staring, M., Pereira, R., Douma, H., van der Neut, J., & Wapenaar, K., 2018. Source-receiver Marchenko redatuming on field data using an adaptive double-focusing method, *Geophysics*, **xx**(y), zz.
- Stolt, R. H., 1978. Migration by Fourier transform, *Geophysics*, **43**(1), 23–48.
- Tellegen, B. D. H., 1948. The gyrator, a new electric network element, *Philips Res. Rep.*, **3**, 81–101.
- Ten Kroode, F., 2002. Prediction of internal multiples, *Wave Motion*, **35**, 315–338.

- Thorbecke, J., Slob, E., Brackenhoff, J., van der Neut, J., & Wapenaar, K., 2017. Implementation of the Marchenko method, *Geophysics*, **82**(6), WB29–WB45.
- van Borselen, R. G., Fokkema, J. T., & van den Berg, P. M., 1996. Surface-related multiple elimination, *Geophysics*, **61**, 202–210.
- van der Neut, J. & Wapenaar, K., 2016. Adaptive overburden elimination with the multidimensional Marchenko equation, *Geophysics*, **21**(5), T265–T284.
- van der Neut, J., Thorbecke, J., Mehta, K., Slob, E., & Wapenaar, K., 2011. Controlled-source interferometric redatuming by crosscorrelation and multidimensional deconvolution in elastic media, *Geophysics*, **76**(4), SA63–SA76.
- van der Neut, J., Vasconcelos, I., & Wapenaar, K., 2015. On Green’s function retrieval by iterative substitution of the coupled Marchenko equations, *Geophysical Journal International*, **203**, 792–813.
- Van der Neut, J., Ravasi, M., Liu, Y., & Vasconcelos, I., 2017. Target-enclosed seismic imaging, *Geophysics*, **82**(6), Q53–Q66.
- Verschuur, D. J., Berkhout, A. J., & Wapenaar, C. P. A., 1992. Adaptive surface-related multiple elimination, *Geophysics*, **57**(9), 1166–1177.
- Wapenaar, C. P. A., 1996. Reciprocity theorems for two-way and one-way wave vectors: a comparison, *Journal of the Acoustical Society of America*, **100**, 3508–3518.
- Wapenaar, C. P. A. & Berkhout, A. J., 1989. *Elastic wave field extrapolation*, Elsevier, Amsterdam.
- Wapenaar, K. & Fokkema, J., 2004. Reciprocity theorems for diffusion, flow and waves, *Journal of Applied Mechanics*, **71**, 145–150.
- Wapenaar, K. & van der Neut, J., 2010. A representation for Green’s function retrieval by multidimensional deconvolution, *Journal of the Acoustical Society of America*, **128**(6), EL366–EL371.
- Wapenaar, K., Fokkema, J., Dillen, M., & Scherpenhuijsen, P., 2000. One-way acoustic reciprocity and its applications in multiple elimination and time-lapse seismics, in *SEG, Expanded Abstracts*, pp. 2377–2380.
- Wapenaar, K., Brogini, F., & Snieder, R., 2012. Creating a virtual source inside a medium from reflection data: heuristic derivation and stationary-phase analysis, *Geophysical Journal International*, **190**, 1020–1024.
- Wapenaar, K., Thorbecke, J., van der Neut, J., Brogini, F., Slob, E., & Snieder, R., 2014. Green’s function retrieval from reflection data, in absence of a receiver at the virtual source position, *Journal of the Acoustical Society of America*, **135**(5), 2847–2861.
- Wapenaar, K., Brackenhoff, J., Thorbecke, J., van der Neut, J., Slob, E., & Verschuur, E., 2018. Virtual acoustics in inhomogeneous media with single-sided access, *Scientific Reports*, **8**, 2497.
- Weglein, A. B., Gasparotto, F. A., Carvalho, P. M., & Stolt, R. H., 1997. An inverse-scattering series method for attenuating multiples in seismic reflection data, *Geophysics*, **62**(6), 1975–1989.
- Weglein, A. B., Araújo, F. V., Carvalho, P. M., Stolt, R. H., Matson, K. H., Coates, R. T., Corrigan, D., Foster, D. J., Shaw, S. A., & Zhang, H., 2003. Inverse scattering series and seismic exploration,

Inverse Problems, **19**, R27–R83.

Williams, E. G. & Maynard, J. D., 1980. Holographic imaging without the wavelength resolution limit, *Physical Review Letters*, **45**, 554–557.

Willis, J. R., 2011. Effective constitutive relations for waves in composites and metamaterials, *Proceedings of the Royal Society A*, **467**, 1865–1879.

Willis, J. R., 2012. The construction of effective relations for waves in a composite, *Comptes Rendus Mecanique*, **340**, 181–192.

Wu, S. F., 2004. Hybrid near-field acoustic holography, *Journal of the Acoustical Society of America*, **115**(1), 207–217.